Original Research Article

Determination of pharmacological impact, therapeutic efficacy and safety profile of *Terminalia chebula* as an antidiabetic hypolipidemic medicine in alloxan-induced diabetic rats

Abstract

Terminalia chebula (*T. chebula*) is a widely used medicinal plant that possesses numerous therapeutic properties, such as antimicrobial, antioxidant, antidiabetic, anti-inflammatory, hepatoprotective, cardioprotective activity. In this study, the ethanolic extract of *T. chebula* was observed to significantly improve the condition of alloxan-induced diabetic rats in a dose-dependent manner. A lower dose (250mg) of *T. chebula* significantly ($p<0.05$) reversed the altered physiological states of alloxan-induced diabetic rats, but a higher dose (650mg) yielded greater therapeutic effects. A dose-dependent restoration was also recorded in the levels of SGPT, SGOT, creatinine, HDL, LDL, and triglyceride in alloxan-induced diabetic rats that received three distinct doses (low, medium, high) of the test extract. Afterward, the diabetes healing potentialities of *T. chebula* were compared to those of commercially available medications. This study revealed that different doses of ethanolic extracts of *T. chebula* fruit had similar therapeutic results in treating hyperglycemia as existing conventional medications. A ligand library of the fruit's constituents was prepared through literature mining, and the antidiabetic activities of the ligands and their ADMET properties were assayed *in silico.* The molecular docking studies indicated that the antidiabetic activity of the extract is likely mediated through the inhibition of α-amylase, α-glucosidase, and dipeptidyl peptidase-IV, but further research on this was deemed necessary. The current study ascertains the antidiabetic potentialities of this medicinal plant and opines that comprehensive *in vivo* and *in vitro* analysis of the constituents be carried out to identify and further develop the actual molecules responsible for antidiabetic activity.

Keywords: Diabetes mellitus, blood glucose, *Terminalia chebula*, lipid profile, alloxan, creatinine

Introduction

Diabetes mellitus is a non-transmissible endocrine, metabolic disorder that is quickly spreading across the world, posing a serious global health concern. According to the World Health Organization (WHO), almost 1 in every 10 individuals have diabetes (Gulam *et al*., 2019). It was evaluated by the International Diabetes Federation (IDF) that approximately 425 million individuals worldwide were afflicted with diabetes in 2017, and the number is anticipated to arrive at 629 million by 2045 (Afsana *et al*., 2019). The higher prevalence of diabetes is associated with rapid urbanization, economic growth, population growth, lack of physical activity, changing lifestyles, and eating habits (Wild *et al*., 2004). Due to deficiency or decreased effectiveness of endogenous insulin, diabetic individuals experience high blood glucose, increased glycated hemoglobin, microvascular (retinopathy, neuropathy, and nephropathy), and macrovascular (heart attack, stroke, and peripheral vascular disease) complications (Gad-Elkareem *et al*., 2019; Patel *et al*., 2011). Diabetes can be managed by the combination of a healthy lifestyle, physical activity, and currently available therapies like insulin and oral antidiabetic drugs such as sulfonylureas, biguanides, and glinides (Patel *et al*., 2012). Even though the current medications are effective in controlling diabetes, they are

not without side effects, which remains a problem with many oral hypoglycemic drugs (Aung *et al*., 2017). For instance, diarrhea, bloating, difficulty in the digestion or absorption of nutrients from food, nausea, vomiting, and headache are all typical side effects of metformin (biguanides) (Mohiuddin *et al*., 2019). Apart from the side effects associated with the synthetic medications, annual health care expenditure for the long-term treatment of diabetes poses a significant financial burden on people with diabetes (Afsana *et al*., 2019).

Medicinal plants are considered as a potential alternative in the treatment of diabetes mellitus (Amalraj & Gopi, 2017). As medicinal plants are widely available resources for primary healthcare, the majority of the world's populations in developing countries continue to rely on them to satisfy their health requirements. They have a wide range of biological and pharmacological actions, as well as better safety margins and cheaper costs (Kannan *et al*., 2012). Bioactive components found in medicinal plants offer a wide range of therapeutic effects. Hence, a single plant may be utilized to treat a variety of illnesses. Moreover, genetic alteration can be used to increase or minimize the concentration of a particular plant component (Ramesh *et al*., 2012).

In Bangladesh, various medicinal plants are utilized to treat diabetes mellitus (DM), including *Allium cepa, Aloe vera, Brassica nigra, Terminalia bellerica, Tamarindus indica, Ocimum sanctum,* etc. (Hasan & Sultana, 2018; Rahman *et al*., 2021).

T. chebula is an important medicinal plant that has been appropriated in the Unani System of Medicine (USM) to treat a variety of ailments and infections since ancient times. *T. chebula* is a medicinal plant extensively disseminated throughout Bangladesh, India, Burma, and Sri Lanka. Haritaki is the traditional Bangla name for this plant, which belongs to the Combretaceae family. In English, Hindi, and Persian, it is known as black myrobalan, Harad, and Halaila, respectively. It is renowned as the "King of Medicines" in Tibet (Basha & Code, 2017; Akhtar & Husain, 2019; Alam *et al*., 2020). It comprises numerous phytochemical constituents such as phenolic acids, tannins, flavonoids, gallic acid, chebulic acid, punicalagin, chebulanin, corilagin, neochebulinic, ellagic acid, chebulegic acid, chebulinic acid, 1,2,3,4,6- Penta-Ogalloyl-ß-D-glucose, 1,6,-di-O-galloyl-D-glucose, casuarinin, 3,4,6-tri-O-galloyl-D-glucose and terchebulin (Nigam *et al*., 2020; Singh & Sheikh, 2020; Das *et al*., 2020; Afshari *et al*., 2016).

It also confers various pharmacological actions such as antidiabetic Activity, anti-inflammatory effect, antibacterial effect, anticancer Activity, antityrosinase Activity, antiaging Activity, antispasmodic Activity, antioxidant Activity, hepatoprotective Activity, nephroprotective Activity, gastroprotective Activity, antihyperlipidemic Activity, hypocholesterolemic Activity, cardioprotective activity, anticonvulsant activity, etc. (Nigam *et al*., 2020; Bag *et al*., 2019; Pugazhendhi *et al*., 2018; Sivamaruthi *et al*., 2019). *Terminalia chebula* root extract plays a significant role as a hypoglycemic agent by restraining α-amylase Activity (Akram *et al*., 2019). Besides its hypoglycemic effect, the hypo-cholesterolemic effect of this plant has also been reported (Anurag Singh *et al*., 2018; Sotoudeh *et al*., 2019). *T. chebula* has also been found to improve the serum lipid profile of diabetic rats with a significant boost in their high-density lipoprotein (HDL) cholesterol levels and a notable fall in their total serum cholesterol, triglycerides, and low-density lipoprotein (LDL) cholesterol levels (Anurag Singh *et al*., 2018). At the same time, this plant has been shown to ameliorate diabetes-induced renal and liver impairment in alloxan diabetic rats (Anurag Singh *et al*., 2018). Consequently, *T. chebula*'s function in the management of diabetes can and is likely to be multifaceted.

In light of the preceding, the current study assesses the pharmacological impact, therapeutic efficacy, reduced side effects, and safety profile of *T. chebula* as an antidiabetic, hypolipidemic medicine in alloxan-induced diabetic rats in a dose and source dependent way.

Method and Materials

Plant Collection and Extract Preparation

The *T. chebula* fruit was obtained from the garden of the Department of Pharmacy, University of Dhaka. The samples were then verified by the University of Dhaka's Department of Pharmacy.

T. chebula fruit was air-dried and roughly pulverized. The powdered fruit was then extracted for some days with 50 % ethanol. The entire mixture was filtered through a new cotton plug, followed by a separate filtering using Whatman No. 1 filter paper every three days. The filtrate liquid was exerted for the following step to lessen the volume using a rotary evaporator at low temperature and pressure. Subsequently, the coarse sediment was used to perform the pharmacological tests that were needed.

Botanical authentication

According to the law of Bangladesh National Herbarium, the samples of all parts of *T. chebula* were deposited, and an accession number (DACB 66285) was allocated as the after identification by the chief scientific officer.

Drugs and Chemicals

The drug and chemicals utilized in this current study m*et al*l of the mandatory analytical standards. Alloxan was purchased from the Sigma Corporation in the United States. Metformin, a standard antidiabetic medicine, was provided as a free sample by Incepta Pharmaceutical Limited. Acetic acid was secured from Chemical.co.uk.

Experimental Animal Procurement, Nursing, and Grouping

A total of 140 male white albino rats weighing within (120-150) gm were purchased from Jahangirnagar University, Savar, Dhaka, Bangladesh. The rats were housed at the University of Dhaka's Institute of Nutrition & Food Science in a climate-controlled setting (temperature 25±3°C, relative humidity 55±5%, and a 12-hour light/dark cycle). The rats had access to conventional chow and clean drinking water and were fed ad libitum. Before the trial, all of the animals were housed in this habitat for at least one week. The Institutional Animals Ethics Committee (IEAC) approved all experimental procedures. One hundred forty rats were continuously distributed to 14 groups of ten rats. In each experiment, rats were chosen at random for each group.

Animal model Sample Size detection

The Power "Analysis Method" was used to calculate the sample size. The equation for this is provided below:

Sample size = $2\ SD^2\ (Z\alpha/2 + Z\beta)^2/d^2$ (Yin *et al*., 2018)

Where Standard deviation = from previous studies or pilot study

$Z\alpha/2 = Z\ 0.05/2 = Z\ 0.025 = 1.96$ (From Z table) at type 1 error of 5%

$Z\beta = Z\ 0.20 = 0.842$ (From Z table) at 80% power

d = effect size = difference between pre-treatment and post-treatment mean values of blood glucose levels

Expected attrition/ death of animals: To account for projected erosion, the final sample size was adjusted. 10% attrition after alloxan administration was observed in earlier studies, and this was accounted for while determining sample size.

Five rats were taken and appropriated as Diabetic Controls in the pilot trial (alloxan-induced group). Five rats were used in each pre-clinical trial based on the aforementioned estimate.

The rats were left undisturbed for four weeks after intra-peritoneal injection of alloxan at a 150 mg/kg body weight dose to raise the blood glucose levels of the subjects significantly

The mean blood glucose level after four weeks was 25.42 mmol/L, with a standard deviation of 5.17.

In accordance with our previously conducted studies, if the mean blood glucose level is 18.58 mmol/L or lower following treatment with the extract, it can be concluded that the plant extract can significantly lower the elevated blood sugar levels ($p<0.05$).
The standard deviation of the Pilot study: 5.17
$Z\alpha/2 = 1.96$, $Z\beta = Z\ 0.20 = 0.842$, d= 25.42-18.58=6.84,
So, Sample size = 2 2 SD^2 $(Z\alpha/2 + Z\beta)^2/d^2$=2× (5.17)2× (1.96+0.842)2/ (25.42-18.58)2 =8.97
This was modified to account for the presumed attrition to obtain the final study group size.
Presumed attrition-adjusted sample size = 8.97/0.9=9.97.
Therefore, the current study was conducted employing ten rats in each experimental group (Charan & Kantharia, 2013).

Dose selection for respective study

An initial pilot study indicated that the pharmacological activity of the test extract (*T. chebula*) was obtained at a minimal dose of 250mg/kg, which placed the minimum effective concentration (MEC) value at above 250mg/kg. Increasing the dose resulted in a more prominent activity until a threshold value of 650mg/kg, at which the receptors responsible for pharmacological action started getting saturated. As a result, the impact did not increase significantly when the dose was raised from 650mg/kg to 1000mg/kg. Moreover, the same procedure was followed to select the doses of the standard drugs.

Evaluation of Antidiabetic Activity

In order to conduct this study,140 rats were randomly selected and evenly divided into fourteen groups.
Chart 1 :

Group Number	Group Specification	Treatment species	Dose Treatment species (mg/kg)	Abbreviation of Groups
1	Negative Control	Physiological Saline	10mL/kg	C
2	Alloxan Control	Alloxan	150mg/kg	A
3	Alloxan+ Metformin	Alloxan+ Metformin	150mg/kg + 100mg/60kg	$A+M_{100}$
4	Alloxan+ Metformin	Alloxan+ Metformin	150mg/kg + 200mg/60kg	$A+M_{200}$
5	Alloxan + Metformin	Alloxan+ Metformin	150mg/kg 400mg/60kg	$A+M_{400}$
6	Alloxan + *T. chebula*	Alloxan + *T. chebula*	150mg/kg + 250 mg/kg	$A+TC_{250}$
7	Alloxan + *T. chebula*	Alloxan + *T. chebula*	150mg/kg + 400 mg/kg	$A+TC_{400}$
8	Alloxan + *T. chebula*	Alloxan + *T. chebula*	150mg/kg + 650 mg/kg	$A+TC_{650}$
9	Metformin	Metformin	100mg/60kg	M_{100}
10	Metformin	Metformin	200mg/60kg	M_{200}
11	Metformin	Metformin	400mg/60kg	M_{400}
12	*T. chebula*	*T. chebula*	250mg/kg	TC_{250}
13	*T. chebula*	*T. chebula*	400mg/kg	TC_{400}
14	*T. chebula*	*T. chebula*	650mg/kg	TC_{650}

In order to induce diabetes, seven groups (2-8) of rats were given alloxan through an intraperitoneal route at a dose of 150 mg/kg body weight (Yin *et al*., 2018). On the contrary, the rats in groups 1 and 9-14 were not given any alloxan. Subsequently, blood glucose levels

of rats in all groups were measured to ascertain the diabetic status after alloxan administration. The duration of the treatment was six weeks, and blood glucose levels of rats were measured once a week during their fasting period. Both the extracts (Alloxan + *T. chebula*) and the drugs were administered orally.

Statistical Analysis

All the findings (raw data) of this study were segmented into different categories based on a wide range of study factors that were documented and evaluated on a broadsheet using Microsoft Excel software. Descriptive statistics were employed for the findings (raw data), and the results were expressed as a mean standard deviation (±SD). The "One Way Anova Test" in SPSS 16 software was used to interpret inter-group heterogeneity in terms of various biological characteristics in order to establish statistical significance. A p-value of less than 0.05 ($p<0.05$) was considered significant for all statistical analyses.

***In silico* molecular docking studies**

A ligand library of 60 constituents of *T. chebula* fruit was prepared through literature mining. 3-dimensional structures of the ligands were downloaded in the sdf format from the 'PubChem' database, and the structures not available were drawn in the 'Avogadro' software package.(Hanwell *et al*., 2012; S. Kim *et al*., 2021) All ligands were optimized under the MMFF94 forcefield using the steepest descent algorithm with the convergence value set to 10e-7 using the 'Avogadro' software package and saved in the pdb format (Halgren, 1996). 4 common antidiabetic drug macromolecular targets, namely α-amylase, AMP-activated protein kinase (AMPK), dipeptidyl peptidase-IV (DPP-IV) and peroxisome proliferator-activated receptor-γ (PPAR-γ) were downloaded from the 'Protein Data Bank' database in the pdb format, their respective PDB IDs being 3OLG, 6C9F, 2G5T, and 4EMA. (Berman *et al*., 2003) The macromolecules were prepared in the 'PyMol' software package, and energy minimization was carried out in vacuo under the 'GROMOS96' forcefield with the 43B1 parameters set using the software package 'Swiss-PdbViewer 4.1.0'.(Guex & Peitsch, 1997; Schrödinger, LLC, 2015; van Gunsteren *et al*., 1996) The 'PyRx' software was used for its AutoDock Vina component, which was used to perform molecular docking (Dallakyan & Olson, 2015). The binding sites were obtained from previous literature and specified in the docking procedure. The results were analyzed and visualized in the software packages' PyMol' and 'Discovery Studio Visualizer 2020'. (Design, 2014; Schrödinger, LLC, 2015) The software 'OpenBabel' was used to obtain the canonical SMILES of the ligands, and the SMILES were used to computationally predict the ADMET properties of the ligands using the webservers' SwissADME' and 'ProTox-II.' (Banerjee *et al*., 2018; Daina *et al*., 2017; O'Boyle *et al*., 2011)

Experimental Guideline

All experiments were carried out in accordance with the Declaration of Helsinki 2013's ethical guidelines. Handling and managing of animals were done in accordance with Swiss Academy of Medical Sciences and Swiss Academy of Sciences guidelines. The latest procedures for the Euthanasia of Animals: 2020 edition were used to euthanize the animals.

Results and Finding

Administration of *T. chebula* resulted in a significant increase in body weight of alloxan-induced diabetic rats **[Figure 1]**. The final step of the experiment revealed an increase in body weight in the negative control group. In the positive control group, alloxan administration led to a drop in final body weight. Both metformin and plant extract reversed the disease condition in a dose-dependent manner, though metformin was observed to show superiority. There were no changes in the normal physiological functions of the healthy rats when they were solely treated with the plant extract, which ensures the safety of using this plant as an antidiabetic medication.

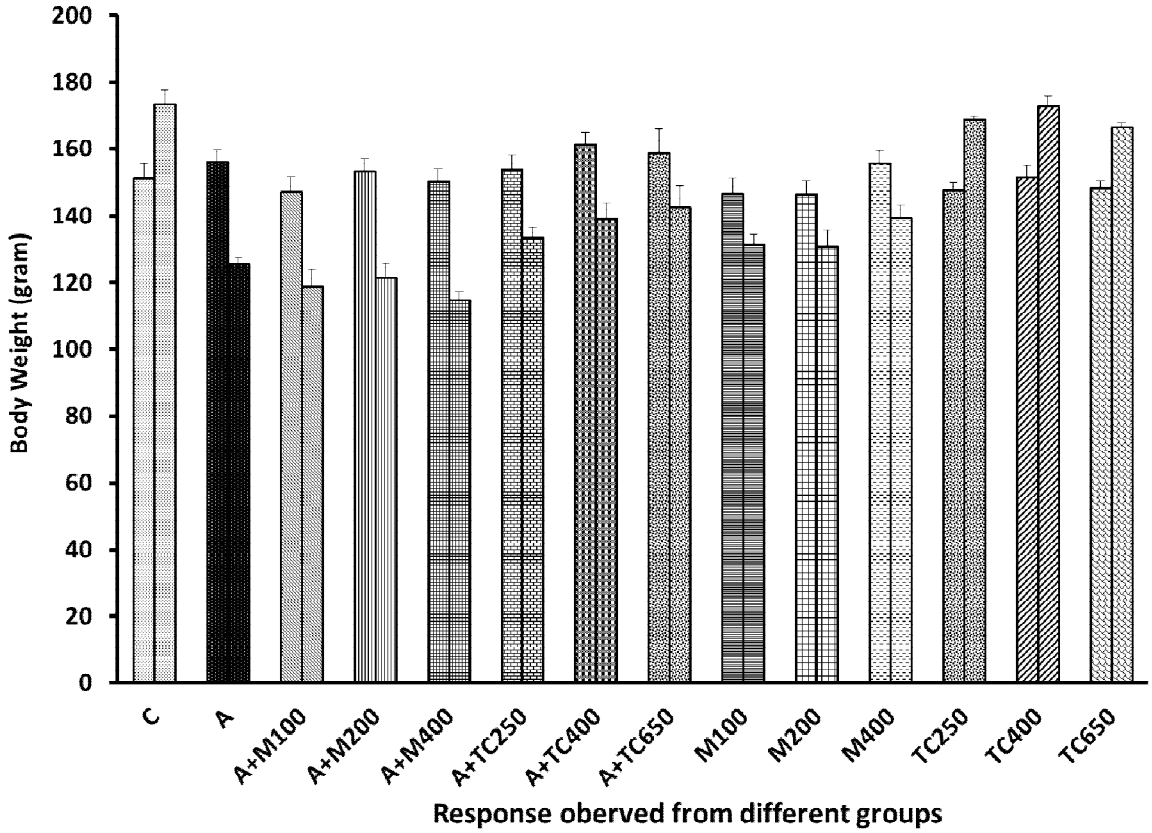

Figure 1: Body weight of rats of 14 groups before and after completing the experiment in diabetic rats. Values were expressed as mean±SD. (C = Control group, A = Alloxan induced group, M = Metformin, A+M = Alloxan + Metformin, A+TC= Alloxan + *Terminalia chebula*, TC= *Terminalia chebula*).

A significant difference between negative control and alloxan-induced groups implied that the disease condition was induced successfully **[Figure 2].** Both metformin and plant extracts successfully decreased the body glucose level in a dose-dependent manner. Treatment of healthy rats with only *T. chebula* expressed a similar curve as the negative control group.

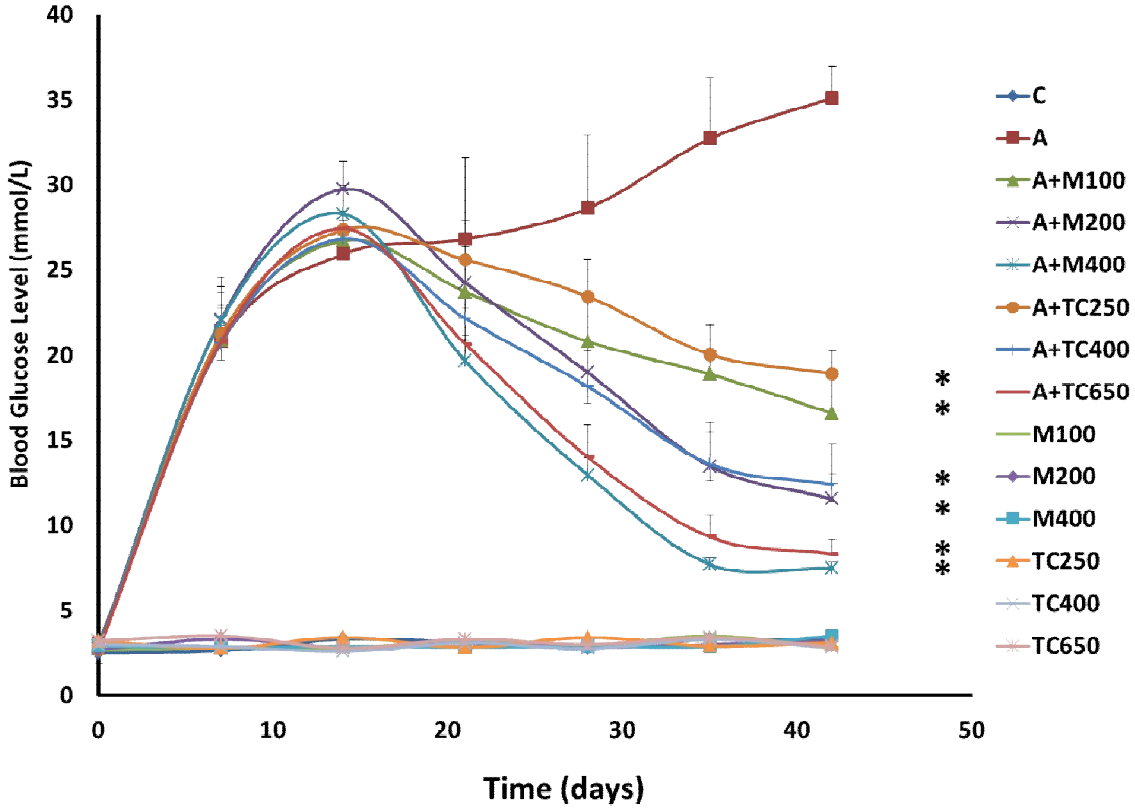

Figure 2: The blood glucose level (mmol/dl) of rats of 14 groups after receiving 42 days of respective treatments. The data were expressed as mean±standard deviation (*indicates statistically significant change).
(C = Control group, A = Alloxan induced group, M = Metformin, A+M = Alloxan + Metformin, A+TC= Alloxan + *Terminalia chebula*, TC= *Terminalia chebula*).

The serum glutamic pyruvic transaminase (SGPT) and serum glutamic-oxaloacetic transaminase (SGOT) levels of the alloxan-treated group were increased to a higher level than that of the negative control. **[Figure 3, Figure 4]** The SGPT and SGOT levels of the positive control and negative control groups were significantly different. They were found significantly higher in diabetic rats treated with *T. chebula* than in diabetic rats treated with metformin.

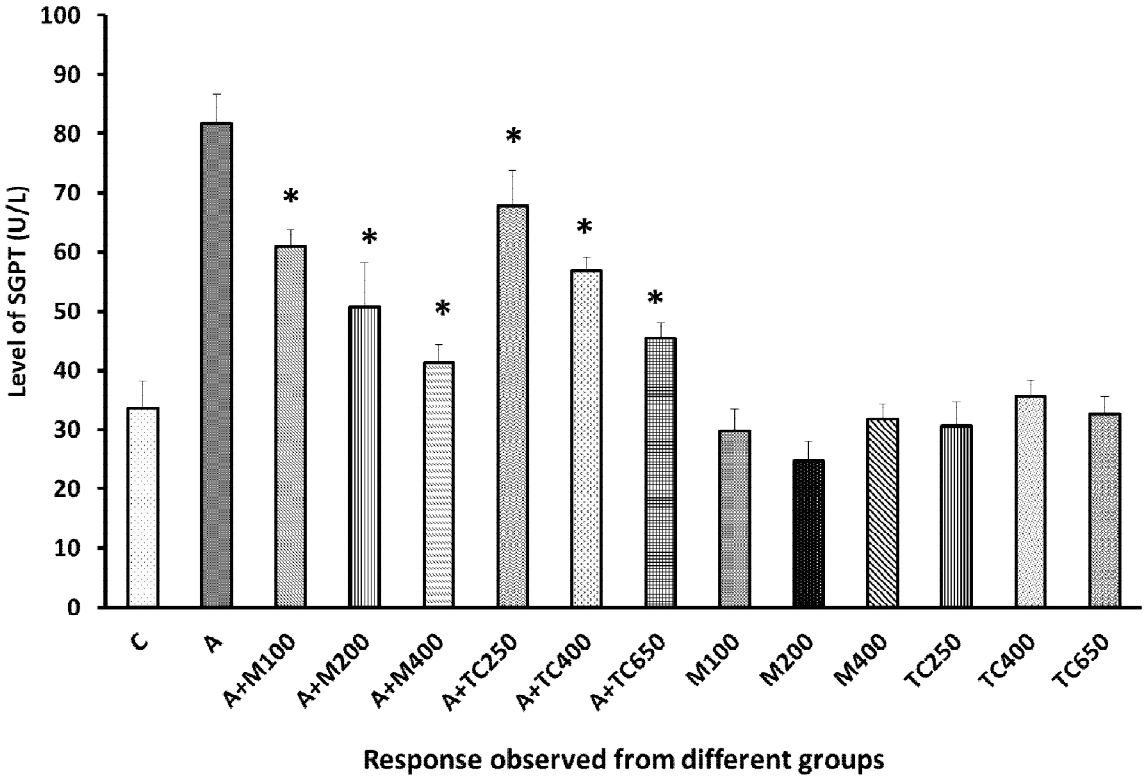

Figure 3: SGPT (U/L) Level of rats from 14 groups. The data were expressed as mean± standard deviation (* indicates statistically significant change). (C = Control group, A = Alloxan induced group, M = Metformin, A+M = Alloxan + Metformin, A+TC= Alloxan + *Terminalia chebula*, TC= *Terminalia chebula*).

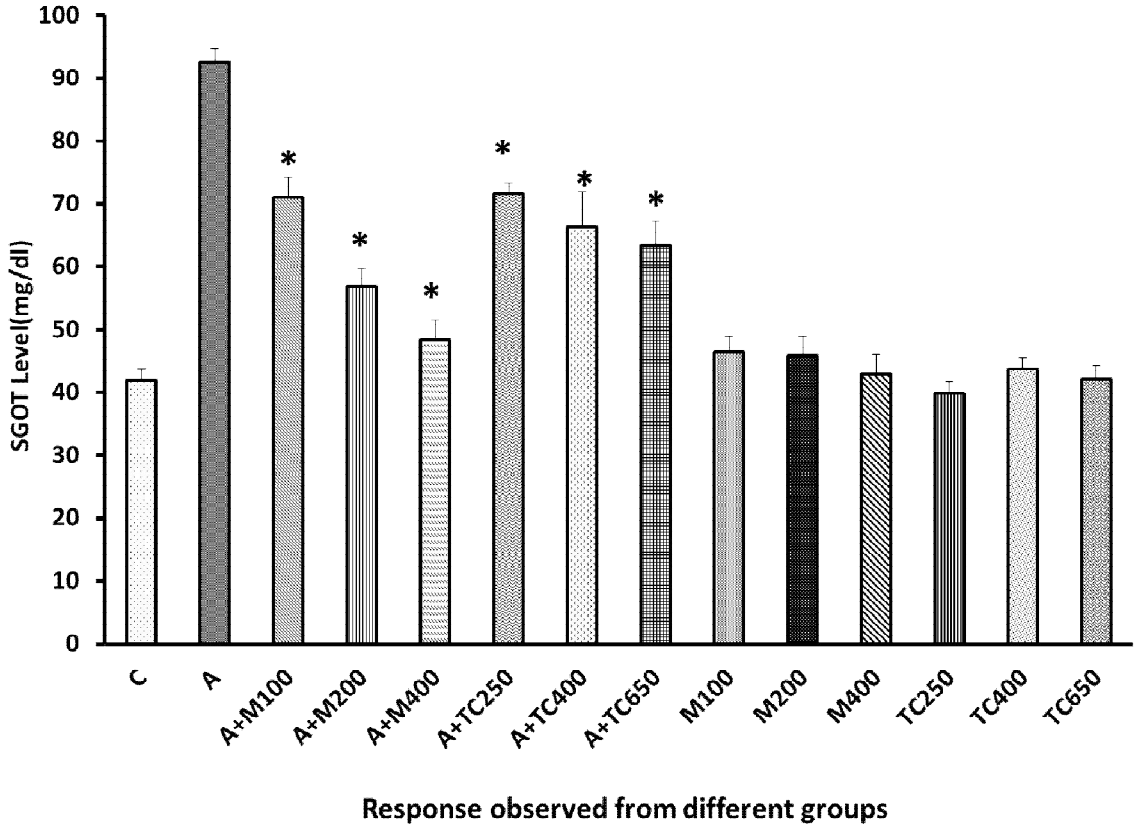

Figure 4: SGOT (U/L) Level of rats from 14 groups. The data were expressed as mean± standard deviation (* indicates statistically significant change). (C = Control group, A = Alloxan induced group, M = Metformin, A+M = Alloxan + Metformin, A+TC= Alloxan + *Terminalia chebula*, TC= *Terminalia chebula*).

Both the standard drug and extract demonstrated statistical significance, confirming the efficacy of *T. chebula e*xtract. [**Figure 5]** There was no significant difference in creatinine levels between the remaining six non-alloxan induced groups and the negative control group.

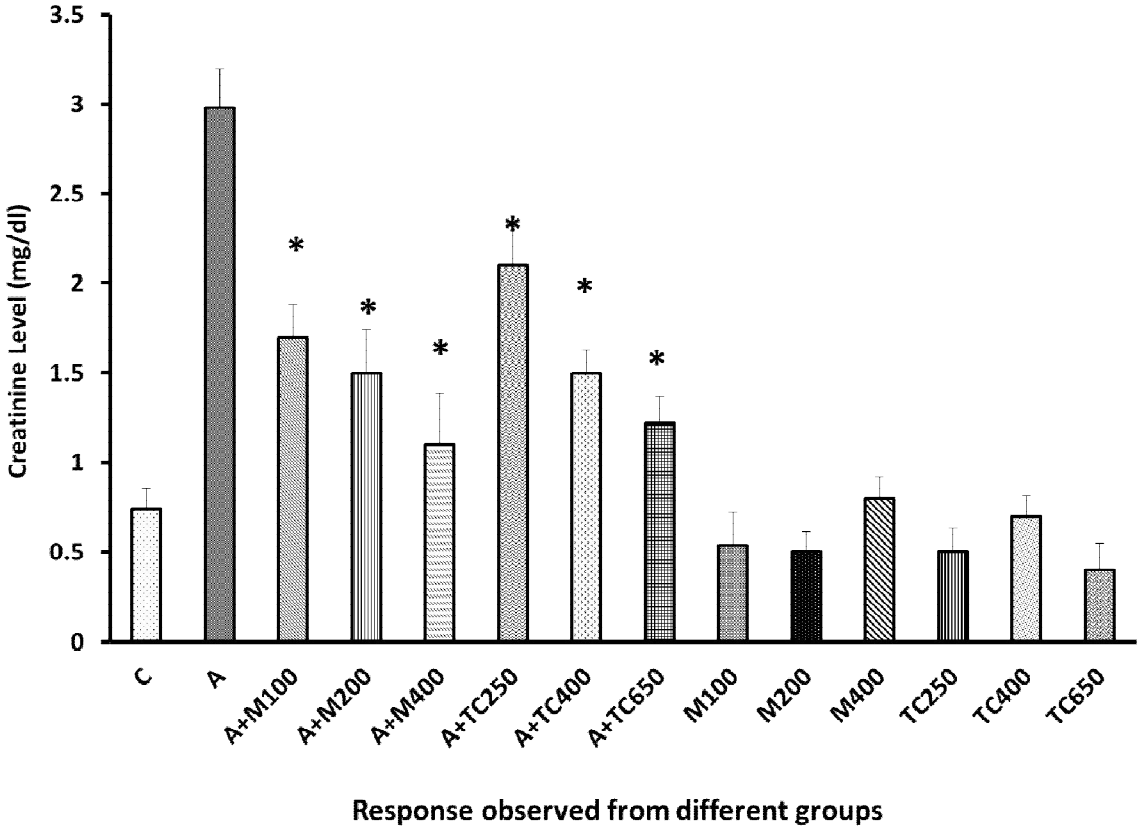

Figure 5: Creatinine (mg/dl) level of rats from 14 groups. The data were expressed as mean± standard deviation (* indicates statistically significant change). (C = Control group, A = Alloxan induced group, M = Metformin, A+M = Alloxan + Metformin, A+TC= Alloxan + *Terminalia chebula*, TC= *Terminalia chebula*).

Alloxan administration successfully increased cholesterol levels in all groups except one (negative control group). **[Figure 6]** Following treatment of diabetic rats with metformin and *T. chebula* extract, a dose-dependent decrease in total cholesterol was observed.

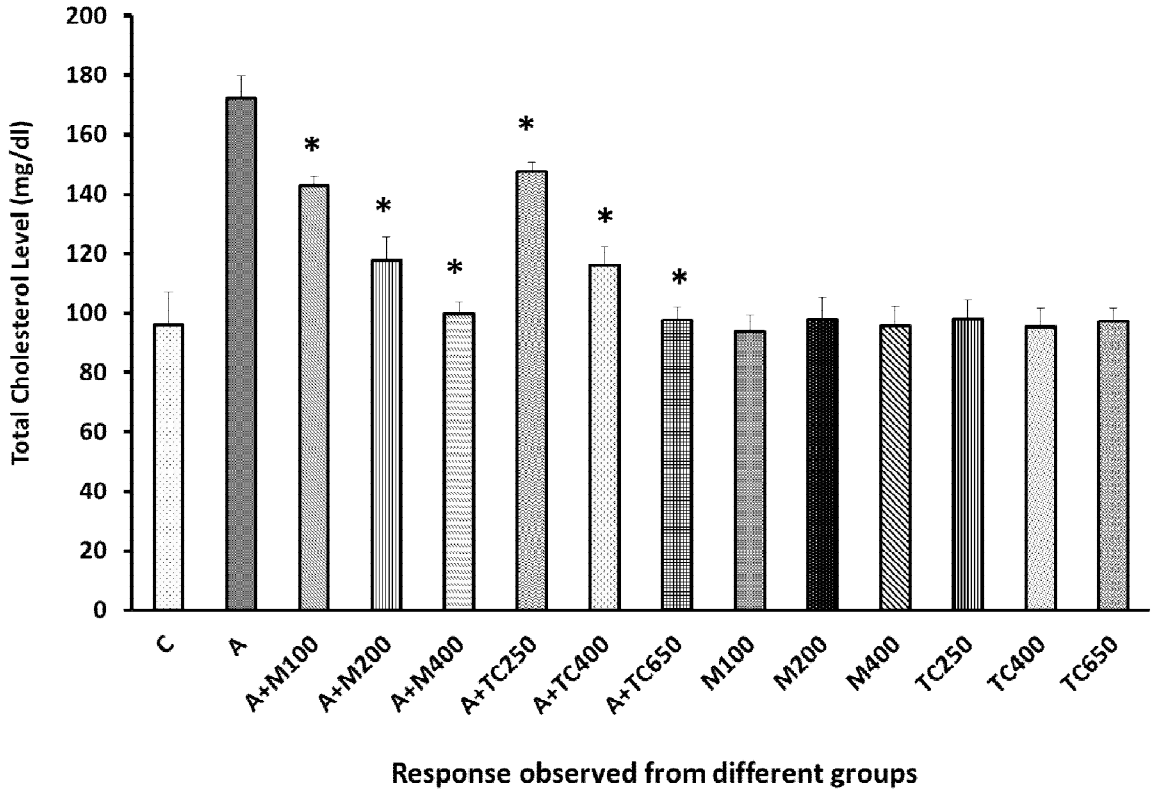

Figure 6: Total Cholesterol (mg/dl) level of rats from 14 groups. The data were expressed as mean± standard deviation (* indicates statistically significant change). (C = Control group, A = Alloxan induced group, M = Metformin, A+M = Alloxan + Metformin, A+TC= Alloxan + *Terminalia chebula*, TC= *Terminalia chebula*).

Diabetes induced a decrease in HDL and plasma periostin levels in diabetic specimens. *T. chebula* extract, like metformin, successfully boosted HDL levels in a dose-dependent manner. **[Figure7]**

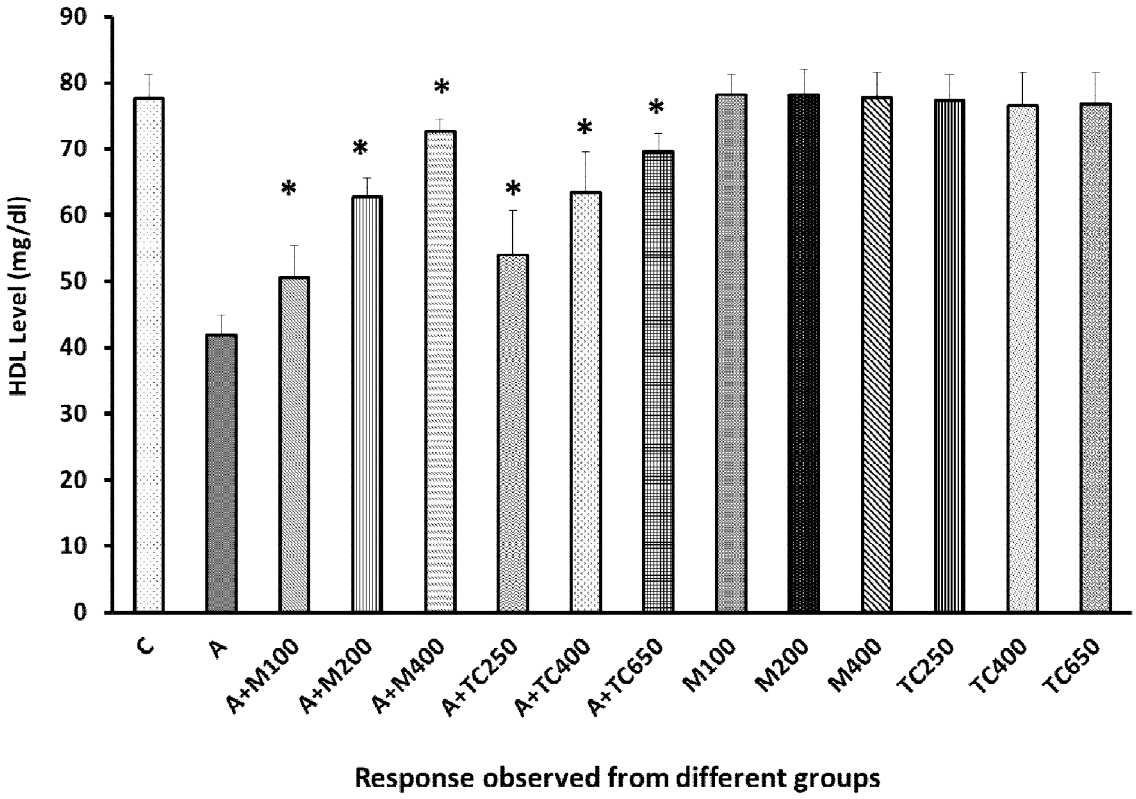

Figure 7: HDL (mg/dl) level of rats from 14 groups. The data were expressed as mean± standard deviation. (* indicates statistically significant change). (C = Control group, A = Alloxan induced group, M = Metformin, A+M = Alloxan + Metformin, A+TC= Alloxan + *Terminalia chebula*, TC= *Terminalia chebula*).

In sharp contrast to the negative control group, the positive control group had a significantly greater amount of LDL after alloxan administration. **[Figure 8]** treatment of diabetic rats with metformin or T. chebula extract at varying dosages efficiently restored normal LDL levels induced by alloxan.

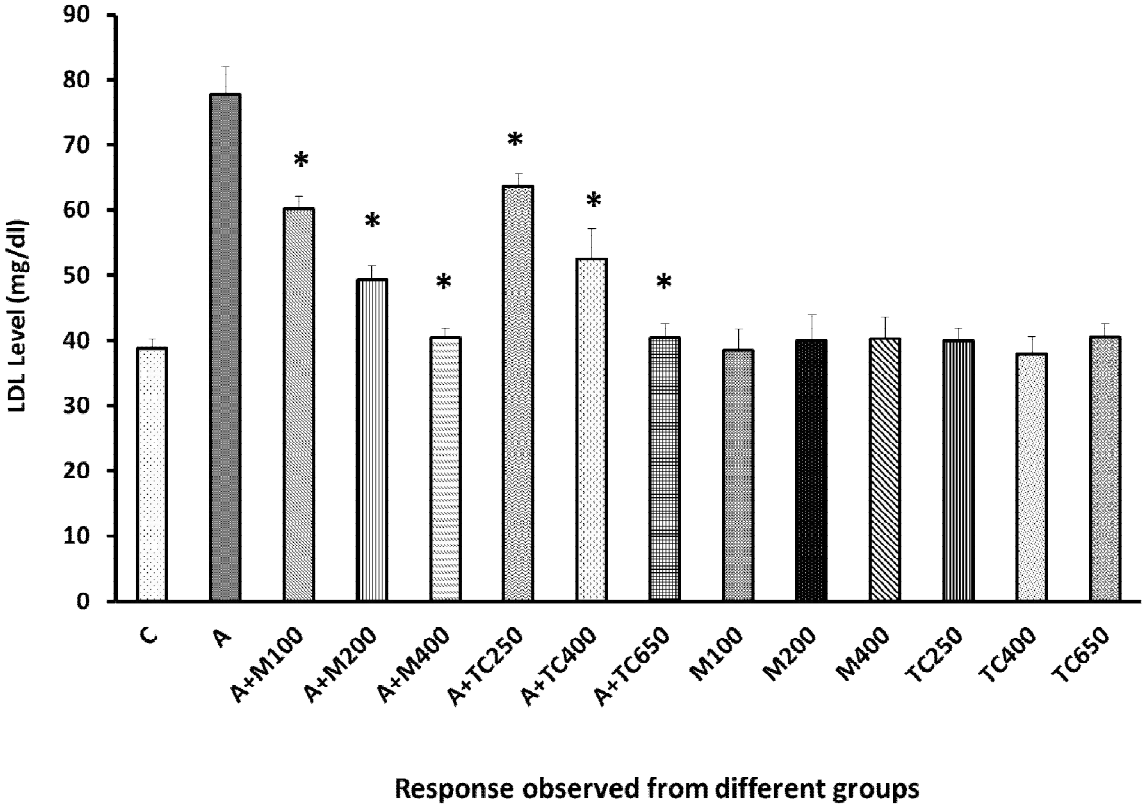

Figure 8: LDL (mg/dl) level of rats from 14 groups. The data were expressed as mean± standard deviation. (* indicates statistically significant change). (C = Control group, A = Alloxan induced group, M = Metformin, A+M = Alloxan + Metformin, A+TC= Alloxan + *Terminalia chebula*, TC= *Terminalia chebula*).

A significant difference in triglyceride levels was seen between the positive and negative control groups, as evidenced by the increased triglyceride levels following alloxan induction [**Figure 9].** Both metformin and plant extract decreased triglyceride levels gradually in a dose-dependent manner.

Figure 9: Triglyceride (mg/dl) level of rats from 14 groups. The data were expressed as mean± standard deviation. (* indicates statistically significant change). (C = Control group, A = Alloxan induced group, M = Metformin, A+M = Alloxan + Metformin, A+TC= Alloxan + *Terminalia chebula,* TC= *Terminalia chebula).*

In silico analysis

The phytoconstituent library comprised of 59 compounds, of which 36 were tannins, 2 were simple phenolic acid derivatives, and 4 were flavonoids. The constituents are presented in Table1.

Table 1: Phytoconstituents of *T. chebula* fruit

Chemical Class	Constituent Name	Pubchem CID	Compound code	Reference
Tannin	1,2,3,4,6-Penta-O-galloyl-β-D-glucose	-	Compound 1	(Juang *et al.*, 2004; Lee *et al.*, 2017)

	1,2,3,6-Tetra-O-galloyl-4-O-cinnamoyl-β-D-glucose	-	Compound 2	(Lee *et al.*, 2017)
	1,2,3,6-Tetra-O-galloyl-β-D-glucose	-	Compound 3	(Lee *et al.*, 2017)
	1,2,3-Tri-O-galloyl-6-O-cinnamoyl-β-D-glucose	-	Compound 4	(Lee *et al.*, 2017)
	1,2,4,6-Tetra-O-galloyl-β-D-glucose	-	Compound 5	(Lee *et al.*, 2017)
	1,2,-Di-O-galloyl-6-O-cinnamoyl-β-D-glucose	-	Compound 6	(Lee *et al.*, 2017)
	1,3,4-Tri-O-galloyl-β-D-glucose	-	Compound 7	(Lee *et al.*, 2017)
	1,3,6-Tri-O-galloyl-β-D-glucose	-	Compound 8	(Lee *et al.*, 2017)
	1,3-Di-O-galloyl-β-D-glucose	-	Compound 9	(Lee *et al.*, 2017)
	1,6-Di-O-galloyl-2-O-cinnamoyl-β-D-glucose	-	Compound 10	(Lee *et al.*, 2017)
	1,6-Di-O-galloyl-β-D-glucose	-	Compound 11	(Juang *et al.*, 2004; Lee *et al.*, 2017)
	1'-O-Methyl neochebulinate	-	Compound 12	(Lee *et al.*, 2017)
	3,4,6-Tri-O-galloyl-D-glucose	-	Compound 13	(Juang *et al.*, 2004)
	4'-epi-neochebulagic acid	-	Compound 14	(Lee *et al.*, 2017)
	4-O-(2",4''-di-O-galloyl-a-L-rhamnosyl) ellagic acid	-	Compound 15	(Lee *et al.*, 2017)
	4-O-(3",4''-Di-O-galloyl-α-L-rhamnosyl)ellagic acid	-	Compound 16	(Lee *et al.*, 2017)
	4-O-(4''-O-Galloyl-α-L-rhamnosyl)ellagic acid	-	Compound 17	(Lee *et al.*, 2017)
	4-O-Galloyl-(-)-shikimic acid	-	Compound 18	(Lee *et al.*, 2017)
	5-O-Galloyl-(-)-shikimic acid	-	Compound 19	(Lee *et al.*, 2017)
	6-O-Galloyl-β-D-glucose	13186191	Compound 20	(Lee *et al.*, 2017)
	6'-O-Methyl chebulate	-	Compound 21	(Lee *et al.*, 2017)
	7'-O-Methyl chebulate	-	Compound 22	(Lee *et al.*, 2017)

	Casuarinin/ Stachyurin	157395	Compound 23	(Juang *et al*., 2004)
	Chebulagic acid	442674	Compound 24	(Juang *et al*., 2004; LIN *et al*., 1990)
	Chebulanin	75034370	Compound 25	(Juang *et al*., 2004)
	Chebulic acid	71308174	Compound 26	(Juang *et al*., 2004)
	Chebulinic acid	72284	Compound 27	(Juang *et al*., 2004; LIN *et al*., 1990)
	Corilagin	73568	Compound 28	(Lee *et al*., 2017; LIN *et al*., 1990)
	Eschweilenol C	10026656	Compound 29	(Lee *et al*., 2017)
	Gemin D	471119	Compound 30	(Lee *et al*., 2017)
	Methyl chebulagate	-	Compound 31	(Lee *et al*., 2017)
	Neochebulagic acid	14483082	Compound 32	(Lee *et al*., 2017)
	Neochebulanin	-	Compound 33	(Lee *et al*., 2017)
	Neochebulinate	-	Compound 34	(Lee *et al*., 2017)
	Phyllanemblinin E	101151868	Compound 35	(Lee *et al*., 2017)
	Phyllanemblinin F	101151869	Compound 36	(Lee *et al*., 2017)
	Punicacortein C	16129720	Compound 37	(Lee *et al*., 2017)
	Punicacortein D	-	Compound 38	(Lee *et al*., 2017)
	Punicalagin	44584733	Compound 39	(Juang *et al*., 2004; Lee *et al*., 2017; LIN *et al*., 1990)
	Tellimagrandin I	442690	Compound 40	(Lee *et al*., 2017)
	Tercatain	14411426	Compound 41	(Lee *et al*., 2017)
	Terchebulin	16175789	Compound 42	(LIN *et al*., 1990)
	Terflavin A	16175788	Compound 43	(Lee *et al*., 2017; LIN *et al*., 1990)
Simple phenolic acid derivatives	4-O-Methylgallic acid	78016	Compound 44	(Anil & Nandini, 2010)
	Caffeic acid	689043	Compound 45	(Tariq & Reyaz, 2013)
	Digallic acid	341	Compound 46	(Lee *et al*., 2017)
	Ellagic acid	5281855	Compound 47	(Lee *et al*., 2017)
	Ethyl gallate	13250	Compound 48	(Anil & Nandini, 2010)
	Eugenol	3314	Compound 49	(H. G. Kim *et al*., 2006)
	Ferulic acid	445858	Compound 50	(Tariq & Reyaz, 2013)
	Gallic acid	370	Compound 51	(Juang *et al*., 2004; Lee *et al*., 2017)
	Melilotic acid	873	Compound 52	(Hosamani, 1994)

	Methyl gallate	7428	Compound 53	(Juang *et al*., 2004; Lee *et al*., 2017)
	p-Coumaric acid	637542	Compound 54	(Tariq & Reyaz, 2013)
	Phloroglucinol	359	Compound 55	(Hosamani, 1994)
	Vanillic acid	8468	Compound 56	(Tariq & Reyaz, 2013)
Flavonoids	Isoquercetin	5280804	Compound 57	(Prakash *et al*., 2012)
	Luteolin	5280445	Compound 58	(Prakash *et al*., 2012)
	Quercetin	5280343	Compound 59	(Kumar *et al*., 2009)
	Rutin	5280805	Compound 60	(Kumar *et al*., 2009)

The macromolecular targets are presented in Table 2.

An extensive literature analysis was conducted to identify suitable antidiabetic macromolecular targets for the study, and 5 molecular targets along with their therapeutic activity providing ligands were selected, the first group as molecular targets and the second as respective controls. The macromolecules and their respective controls are presented in table 2.

Table 2: Macromolecular targets for antidiabetic drugs

Macromolecule Name	PDB ID	Control drug	Binding pocket	Reference
α-Amylase	3OLG	Acarbose	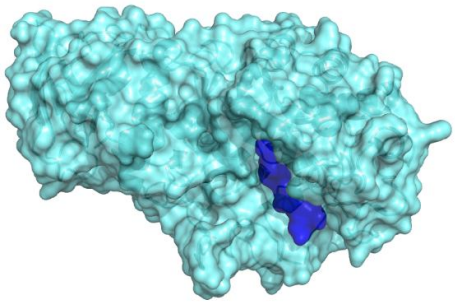	(Shivanagoudra *et al*., 2019)
α-Glucosidase	2ZE0	Acarbose	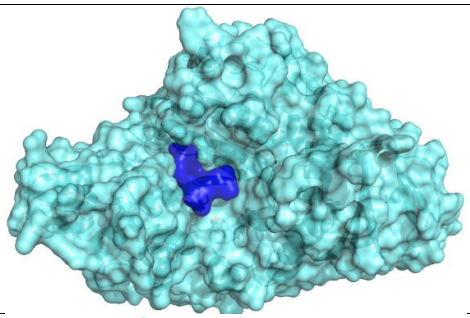	(Jhong *et al*., 2015)
AMP-activated protein kinase	6C9F	PT1	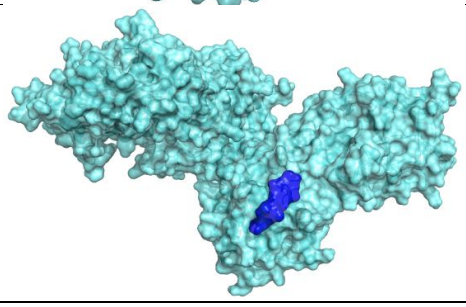	(Pang *et al*., 2008)

Dipeptidyl peptidase IV	2G5T	Sitagliptin	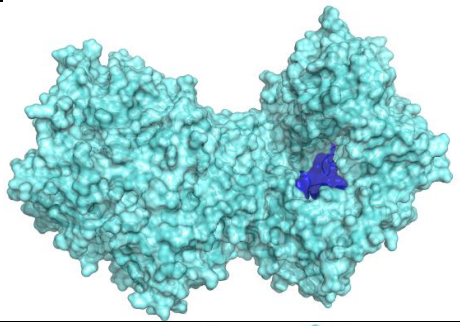	(Nabeno *et al.*, 2013)
Peroxisome proliferator-activated receptor-γ	4EMA	Rosiglitazone	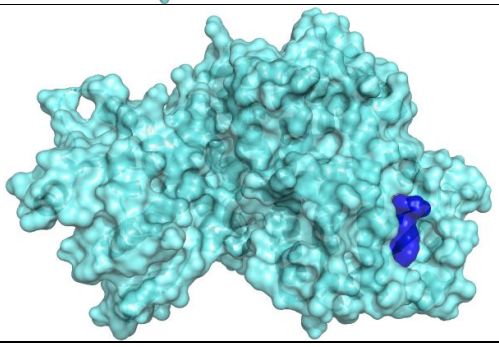	(Sawant *et al.*, 2018)

34 ligands out of 60 displayed higher binding affinity than the control acarbose with α-amylase (3OLG) in the molecular docking studies. The top seven compounds displaying higher binding affinity than acarbose (-7.9) were all tannins, with compound 17 displaying the highest binding affinity (-11.1). Most ligands shared common amino acid interaction residues with the control. These data are presented in table 3.

Table 3: Interaction of ligand library with α-amylase (3OLG)

Ligand	Binding Affinity	Interaction type	Interaction residues
Acarbose	-7.9	Conventional H bond, Carbon - hydrogen bond, Pi-alkyl	THR 163*, TRP 59*, HIS 201*
C17	-11.1	Conventional H bond, Carbon - hydrogen bond, Pi-sigma, Pi-Pi stacked, Pi-Pi T-shaped, alkyl, Pi-alkyl	TRP 58, TRP 59*, GLN 63, ALA 198, ASP 197, ASP 300, ARG 195, ILE 235, GLU 233, HIS 201*, HIS 101, LEU 165, LEU 162
C16	-10.9	Conventional H bond, Carbon - hydrogen bond, Pi- donor hydrogen bond, Pi-sigma, Pi-Pi stacked, Pi-Pi T-shaped, Pi-alkyl	ASP 300, GLN 63, HIS 305, TYR 62, GLY 104, ALA 198, LEU 162, ILE 235, HIS 201*, TYR 151, LYS 200
C15	-10.3	Conventional H bond, Carbon - hydrogen bond, Pi-anion, Pi-Pi stacked, Pi-alkyl	ASN 53, HIS 305, HIS 101, ARG 195, GLU 233, GLY 306, THR 163*, ASP 197, TRP 59*, ALA 198
C29	-9.9	Conventional H bond, Pi-sigma, Pi-Pi T-shaped, Pi-alkyl	GLU 233, LYS 200, TRP 59*, LEU 162, HIS 201*, ALA 198, HIS 305
C5	-9.9	Conventional H bond, Carbon - hydrogen bond, Pi-anion, Pi-Pi stacked, Pi-alkyl	GLY 304, GLY 306, HIS 299, HIS 305, ASP 197, TRP 59*, TYR 62, LEU 162, ILE 235

C10	-9.8	Conventional H bond, Carbon - hydrogen bond, Pi-anion, Pi-sigma, Pi-Pi stacked, Pi-Pi T-shaped, Pi-alkyl	ASP 300, ASP 197, GLU 233, ILE 235, ALA 198, TRP 59*, TYR 62, HIS 201*, LEU 165, LYS 200
C6	-9.5	Conventional H bond, Carbon - hydrogen bond, Pi-anion, Pi-sigma, Pi-Pi stacked, Pi-Pi T-shaped, Pi-alkyl	ARG 195, ASP 300, HIS 299, LYS 200, GLY 306, ASP 197, ILE 235, TYR 62, HIS 201*, LEU 165
C58	-9.4	Conventional H bond, Pi-Pi stacked	ASP 197, GLN 63, TYR 62, TRP 59*
C59	-9.4	Conventional H bond, Pi-Pi stacked	GLN 63, TYR 62, TRP 59*
C8	-9.4	Conventional H bond, Carbon - hydrogen bond, Pi-anion, Pi-donor hydrogen bond, Pi-Pi stacked, Pi-alkyl	TYR 151, HIS 201*, GLY 306, GLU 233, THR 163*, ALA 198, HIS 101, HIS 299, ASP 300, ARG 195, TYR 62, LEU 162, GLY 104
C25	-9.3	Conventional H bond, Carbon - hydrogen bond, Pi-anion, Pi-Pi stacked	HIS 101, HIS 299, ASP 197, ASP 300, ASP 356, GLU 233, GLY 304, THR 163*, HIS 305
C40	-9.3	Carbon-hydrogen bond, Pi-anion	THR 163*, TYR 151, HIS 299, ASP 300, ASP 197, GLU 233
C1	-9.2	Conventional H bond, Carbon - hydrogen bond, Pi-donor hydrogen bond, Pi-Pi stacked, Pi-alkyl	TRP 59*, ASP 356, GLU 233, TYR 151, HIS 299, HIS 305, TYR 62, LEU 162
C2	-9.2	Conventional H bond, Pi-donor hydrogen bond, Pi-sigma, Pi-Pi stacked, Pi-Pi T-shaped	ASP 300, ASP 356, GLU 233, HIS 305, GLY 304, GLN 63, TYR 62, TRP 59*, HIS 201*, LEU 162
C13	-9.1	Conventional H bond, Carbon - hydrogen bond, Pi-sigma, Pi-Pi stacked, Pi-Pi T-shaped, Pi-alkyl	ILE 235, ASP 300, TYR 62, HIS 101, THR 163*, HIS 305, HIS 201*, TRP 59*, LEU 165
C3	-9.1	Conventional H bond, Carbon - hydrogen bond, Pi-Pi stacked, Pi-alkyl	ASP 197, HIS 299, TYR 151, GLU 233, GLY 306, GLN 63, HIS 101, TYR 62, TRP 59*, LEU 162
C4	-9.1	Conventional H bond, Carbon - hydrogen bond, Pi-anion, Pi-Pi stacked, Pi-Pi T-shaped, Pi-alkyl	HIS299, HIS 305, HIS 201*, ASP 300, GLU 233, THR 163*, ASP 197, TYR 62, TRP 59*, LEU 162, ILE 51, ALA 198
C28	-9	Conventional H bond, Carbon - hydrogen bond, Pi-Pi stacked	GLY 306, ASP 300, GLN 63, HIS 305, TRP 59*
C41	-9	Conventional H bond, Pi-anion, Pi-Pi stacked	THR 163*, ASP 300, HIS 305
C60	-9	Conventional H bond, Pi-Pi T-shaped, alkyl, Pi-alkyl	TRP 59*, GLN 63, ASP 300, ILE 235, HIS 201*, LYS 200, LEU 165
C34	-8.9	Conventional H bond, Carbon -	HIS 299, ASP 300, GLN 63,

		hydrogen bond, Pi-sigma, Pi-Pi stacked, Pi-Pi T-shaped, Pi-alkyl	GLY 306, HIS 101, HIS 201*, TYR 62, LEU 162
C11	-8.7	Conventional H bond, Pi-anion, Pi-Pi stacked, Pi-alkyl	GLN 63, HIS 101, GLU 233, ASP 197, TYR 62, LEU 162
C7	-8.6	Conventional H bond, Carbon - hydrogen bond, Pi-anion, Pi-sigma, Pi-Pi T-shaped, Pi-alkyl	GLN 63, THR 163*, ASP 197, ASP 300, GLU 233, HIS 305, GLY 306, ALA 198, ILE 235, HIS 201*, LEU 162, LEU 165
C36	-8.5	Conventional H bond, Carbon - hydrogen bond, Pi-Pi stacked, Pi-alkyl	GLY 306, HIS 299, ASP 300, ASP 197, GLU 233, HIS 305, TYR 151, TYR 62, ILE 235
C9	-8.5	Conventional H bond, Pi-anion, Pi-Pi stacked, Pi-alkyl	GLY 306, ASP 300, HIS 101, HIS 299, HIS 305, ARG 195, GLU 233, ASP 197, TYR 62, ALA 198, LEU 162
C31	-8.4	Conventional H bond, Carbon - hydrogen bond, Pi-anion, Pi-alkyl	ASP 197, GLU 233, THR 163*, TYR 151, HIS 305, GLY 306, ASP 300, LEU 162, LEU 165
C12	-8.3	Conventional H bond, Carbon - hydrogen bond, Pi-anion, Pi-sigma, Pi-Pi stacked	GLU 233, ASP 300, THR 163*, TYR 151, GLN 63, GLY 306, HIS 305, ASP 197, ILE 235, TYR 62, TRP 59*
C14	-8.3	Conventional H bond, Carbon - hydrogen bond, Pi-anion, Pi-Pi stacked	ASP 197, HIS 305, THR 163*, TYR 62
C18	-8.3	Conventional H bond, Pi-donor hydrogen bond, Pi-anion, Pi-Pi stacked, Pi-alkyl	ASP 197, TYR 62, TRP 59*
C30	-8.3	Conventional H bond, Carbon - hydrogen bond, Pi-Pi T-shaped, Pi-alkyl	GLN 63, GLY 306, GLU 233, HIS 305, TYR 62, TRP 59*, LEU 162
C33	-8.3	Conventional H bond, Carbon - hydrogen bond, Pi-sigma	ASP 300, TYR 62, ARG 195, HIS 101, TRP 59*, LEU 162
C46	-8.3	Conventional H bond, Pi-donor hydrogen bond, Pi-anion, Pi-Pi stacked	GLN 63, GLU 233, ASP 300, ASP 197, TYR 62, TRP 59*
C47	-8.3	Conventional H bond, Pi-anion, Pi-Pi T-shaped, Pi-alkyl	HIS 101, HIS 305, GLY 306, TYR 62, LEU 162, ASP 300

*Interactions common with the control

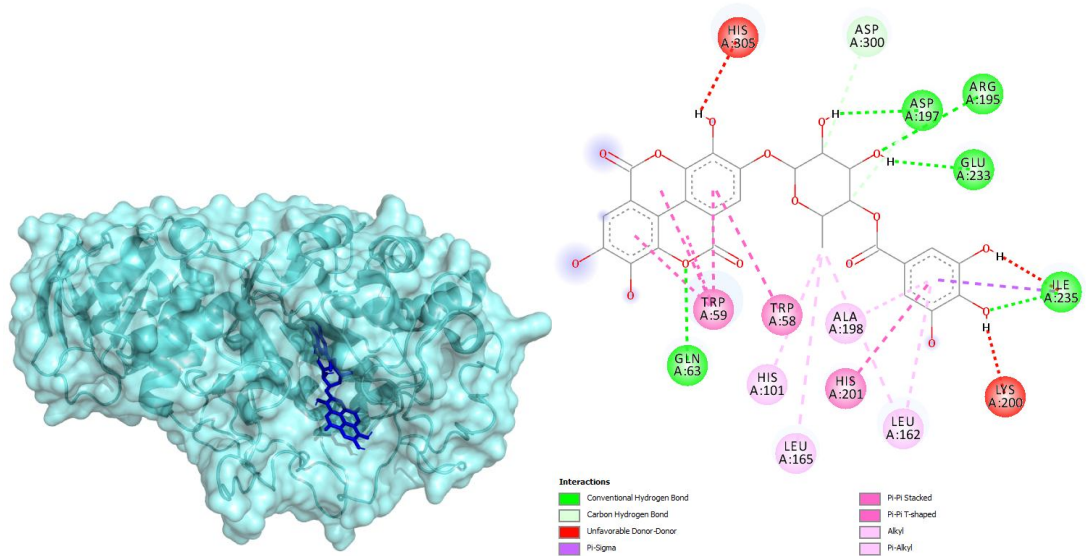

Compound 17

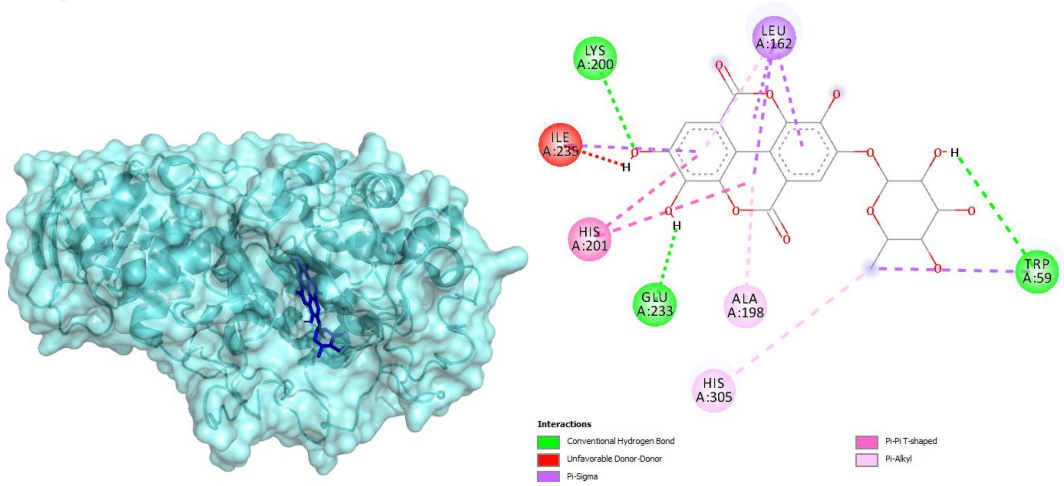

Compound 29

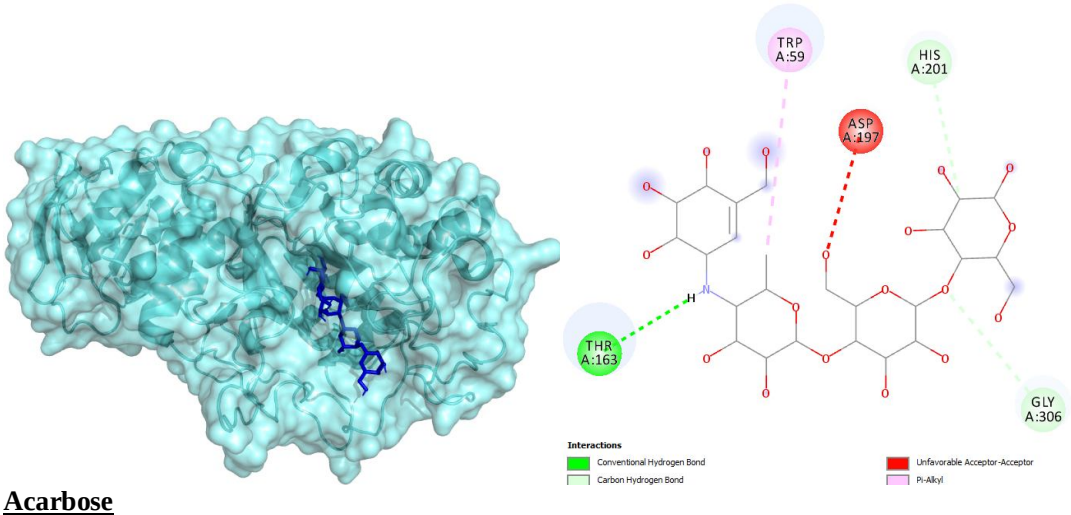

Acarbose

Figure 10: Interaction and binding pose of ligands and control with α-Amylase (3OLG)

44 ligands out of 60 displayed higher binding affinity than the control acarbose with α-glucosidase (2ZE0) in the molecular docking studies. The tannins yet again performed well in

this study, with the top fourteen ligands displaying higher binding affinity than the control all belonging to this group. Compound 2 displayed the highest binding affinity at -10.5 (acarbose: -7.3). Compounds 15,12,28 and 13 displayed high binding affinities (-10, -9.7, -9.5, and -9.4 respectively) compared to the control acarbose (-7.3) but displayed no common interacting residues. These data are presented in table 4.

Table 4: Interaction of ligand library with α-glucosidase (2ZE0)

Ligand	Binding Affinity	Interaction type	Interacting residues
Acarbose	-7.3	Conventional H bond, Carbon hydrogen bond	ASP 326*, GLU 256*
C2	-10.5	Conventional H bond, Pi-cation, Pi-anion, Pi-Pi stacked, Pi-alkyl	HIS 203, ASN 258, ASP 382, ARG 411, ASP 326*, ARG 197, ARG 407, TYR 63, PHE 282, ALA 200, ILE 143
C39	-10.3	Conventional H bond, Carbon hydrogen bond, Pi-anion, Pi-donor hydrogen bond, Pi-Pi T shaped, Pi-alkyl	GLN 167, HIS 203, PHE 282, ILE 143, TYR 63, GLU 256*, ASN 258, ASP 326*, PHE 144, ALA 200
C15	-10	Conventional H bond, Pi-sigma, Pi-Pi stacked, Pi-alkyl	ASP 60, HIS 203, LEU 285, ILE 143, TYR 63, PHE 282
C42	-10	Conventional H bond, Carbon hydrogen bond, Pi-cation, Pi-Pi T shaped, Pi-alkyl	ARG 407, ASP 326*, THR 405, GLU 256*, PHE 282, SER 384, PHE 225, ILE 143, LEU 285, LEU 327
C6	-10	Conventional H bond, Pi-cation, Pi-Pi stacked	ASN 258, GLU 256*, GLN 167, ASN 61, ARG 411, SER 384, ARG 407, TYR 63, PHE 163, PHE 282
C8	-10	Conventional H bond, Pi-cation, Pi-anion, Pi-donor hydrogen bond, Pi-Pi stacked, Pi-alkyl	SER 384, ARG 411, ASP 326*, ASN 324, ALA 200, ASP 199, GLN 167, HIS 325, ARG 197, GLU 256*, ARG 407, TYR 63, PHE 163
C27	-9.9	Conventional H bond, Carbon hydrogen bond, Pi-cation, Pi-anion, Pi-donor hydrogen bond, Pi-Pi stacked, Pi-Pi T shaped, Pi-alkyl	HIS 203, ASN 258, ASP 382, ARG 411, ASP 326*, ARG 197, ARG 407, TYR 63, PHE 282, ALA 200, ILE 143
C34	-9.9	Conventional H bond, Pi-cation, Pi-Pi stacked, Pi-Pi T shaped	ASP 60, HIS 325, TYR 63, ASP 326*, ARG 407, ARG 197, GLU 256*, PHE 282, ASN 258, HIS 203, ALA 200
C40	-9.9	Conventional H bond, Pi-cation, Pi-anion, Pi-donor hydrogen bond, Pi-Pi stacked, Pi-Pi T shaped, Pi-alkyl	GLU 256*, ASP 326*, ARG 407, ASP 382, ASN 324, PHE 282, ALA 200, PHE 163
C1	-9.8	Conventional H bond, Carbon hydrogen bond, Pi-cation, Pi-anion, Pi-donor hydrogen bond, Pi-Pi stacked, Pi-alkyl	SER 384, GLN 167, TYR 63, ASN 324, PHE 282, ASP 326*, ARG 407, ARG 411, PHE 163, HIS 325, LEU 285, ARG 197, GLU 256*
C16	-9.8	Conventional H bond, Pi-cation, Pi-sigma, Pi-Pi stacked, alkyl, Pi-alkyl	SER 384, ASP 326*, ASP 60, ARG 407, PHE 144, TYR 63, PHE 282, ALA 200, LEU 285
C24	-9.8	Conventional H bond, Carbon	ILE 143, ARG 407, ARG 197, ASN

		hydrogen bond, Pi-cation, Pi-anion, Pi-Pi stacked,	324, PHE 282, PHE 144, ASN 258, GLU 256*, HIS 325
C12	-9.7	Conventional H bond, Pi-cation, Pi-sulfur, Pi-Pi stacked	ASN 324, ARG 407, ASP 382, ARG 411, ASP 60, ASN 61, GLN 167, ASN 258, HIS 203, PHE 282, PHE 163, TYR 63, MET 229
C17	-9.7	Conventional H bond, Carbon hydrogen bond, Pi-cation, Pi-anion, Pi-Pi stacked	ASN 258, ASN 324, HIS 325, SER 384, ARG 197, ARG 407, GLU 256*, ASP 326*, PHE 144, PHE 282
C60	-9.7	Conventional H bond, Pi-cation, Pi-anion, Pi-Pi T shaped, Pi-alkyl	GLN 167, HIS 325, ASP 326*, ASN 324, HIS 203, ARG 197, GLU 256*, ALA 200, PHE 163
C10	-9.5	Conventional H bond, Pi-Pi stacked	ARG 411, ASP 326*, GLU 256*, TYR 63, PHE 282
C28	-9.5	Conventional H bond, Pi-cation, Pi-donor hydrogen bond, Pi-Pi stacked,	ASP 60, GLN 167, ILE 143, ASN 61, ARG 411, ARG 407, PHE 163, TYR 63
C7	-9.5	Conventional H bond, Carbon hydrogen bond, Pi-cation, Pi-anion, Pi-Pi T shaped, Pi-alkyl	ASP 199, ALA 200, HIS 325, GLU 256*, ASP 326*, PHE 163, ILE 143
C11	-9.4	Conventional H bond, Carbon hydrogen bond, Pi-cation, Pi-anion	ARG 411, ASN 61, GLN 167, HIS 103, ALA 200, TYR 63, ARG 407, ASP 326*, HIS 325, ARG 197, GLU 256*
C13	-9.4	Conventional H bond, Carbon hydrogen bond, Pi-Pi stacked, Pi-alkyl	HIS 203, ASN 258, ASN 324, ASP 199, GLN 167, TYR 63, PHE 282
C25	-9.4	Conventional H bond, Carbon hydrogen bond	ASN 258, HIS 203, ASP 326*, ARG 407, SER 384, GLU 256*
C31	-9.4	Conventional H bond, Pi-cation, Pi-alkyl	ALA 257, ASN 324, GLU 256*, ARG 197, ARG 387, ARG 407, HIS 325
C4	-9.4	Conventional H bond, Pi-cation, Pi-anion, Pi-Pi stacked	ASP 326*, ASP 199, ASP 98, SER 384, ARG 387, HIS 325, ARG 197, GLU 256*, PHE 144, PHE 282
C9	-9.4	Conventional H bond, Carbon hydrogen bond, Pi-Pi stacked	ASP 326*, HIS 325, ASN 324, TYR 63, ALA 200, GLN 167, PHE 163, PHE 282
C32	-9.3	Conventional H bond	THR 405, ARG 407, GLN 167
C41	-9.3	Conventional H bond, Pi-Pi stacked	HIS 203, ASN 61, TYR 63
C58	-9.3	Conventional H bond, Pi-Pi stacked	ALA 200, ASP 199, ARG 197, ARG 411, ASP 382, TYR 63
C3	-9.2	Conventional H bond, Pi-cation, Pi-anion, Pi-Pi stacked, Pi-Pi T shaped, Pi-alkyl	HIS 203, ASN 258, ASP 382, ARG 411, ASN 324, ARG 407, ARG 197, ASP 326*, PHE 163, PHE 282, ILE 143, ALA 200
C5	-9.1	Conventional H bond, Carbon hydrogen bond, Pi-cation, Pi-anion, Pi-donor hydrogen bond, Pi-Pi stacked	ARG 407, ARG 411, GLN 167, ALA 200, ASP 326*, ASP 199, GLU 256*, HIS 325
C47	-9	Conventional H bond, Pi-Pi stacked	GLN 167, ASP 60, ASP 199, ASP 326*, HIS 325, ARG 411, TYR 63
C29	-8.9	Conventional H bond, Carbon hydrogen bond, Pi-cation, Pi-	ASP 199, HIS 325, TYR 63, PHE 144, ASP 326*

		anion, Pi-Pi stacked, Pi-Pi T shaped	
C38	-8.9	Conventional H bond, Pi-cation, Pi-sigma, Pi-alkyl	THR 405, ARG 407, ASP 326*, LEU 285, LEU 327
C59	-8.9	Conventional H bond, Carbon hydrogen bond, Pi-cation, Pi-anion, Pi-Pi stacked, Pi-Pi T shaped, Pi-alkyl	PHE 163, HIS 103, ARG 197, TYR 63, ALA 200, ASP 326*, GLU 256*, HIS 325
C36	-8.8	Conventional H bond, Pi-Pi stacked	TYR 63, ASN 258, GLN 167, PHE 282
C37	-8.8	Conventional H bond, Carbon hydrogen bond, Pi-cation, Pi-anion, Pi-Pi T shaped	ARG 407, ASN 258, PHE 144, ASP 326*, PHE 282
C30	-8.7	Conventional H bond, Pi-cation, Pi-Pi stacked, Pi-Pi T shaped	ARG 197, ASN 258, ALA 200, ARG 407, PHE 144, PHE 163, PHE 282
C14	-8.6	Conventional H bond, Pi-cation, Pi-anion, Pi-Pi stacked	ARG 387, ARG 407, ASN 258, ALA 200, GLN 167, GLU 256*, ASP 326*, TYR 63, PHE 163
C33	-8.5	Conventional H bond, Pi-anion, Pi-alkyl	ARG 411, ASN 61, ASP 326*, ARG 407, HIS 325, HIS 103, LEU 327
C35	-8.5	Conventional H bond, Pi-anion, Pi-Pi stacked, Pi-Pi T shaped	ARG 407, ASP 326*, GLU 256*, ASN 258, TYR 63, PHE 282
C57	-8.5	Conventional H bond, Carbon hydrogen bond, Pi-cation, Pi-anion, Pi-Pi stacked, Pi-alkyl	GLN 167, ALA 200, PHE 163, TYR 63, ASP 326*, GLU 256*, HIS 325
C19	-8.4	Conventional H bond, Pi-Pi stacked, Pi-alkyl	ASP 60, ALA 200, ASP 98, ASP 326*, ARG 197, TYR 63
C18	-8.1	Conventional H bond, Pi-Pi stacked	ARG 197, ASN 324, ALA 200, HIS 103, GLN 167, PHE 163, TYR 63
C46	-8.1	Conventional H bond, Carbon hydrogen bond, Pi-cation, Pi-donor hydrogen bond, Pi-Pi stacked	ARG 411, GLN 167, PHE 163, HIS 103, TYR 63, ARG 407
C20	-7.9	Conventional H bond, Carbon hydrogen bond, Pi-Pi stacked	ARG 411, ASP 326*, HIS 325, GLU 256*, TYR 63, ASP 60

*Interactions common with the control

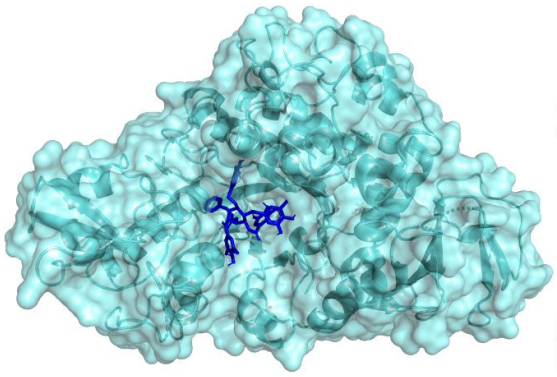

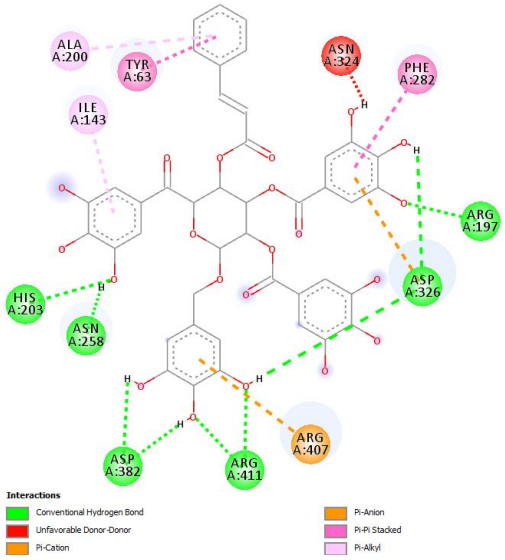

Compound 2

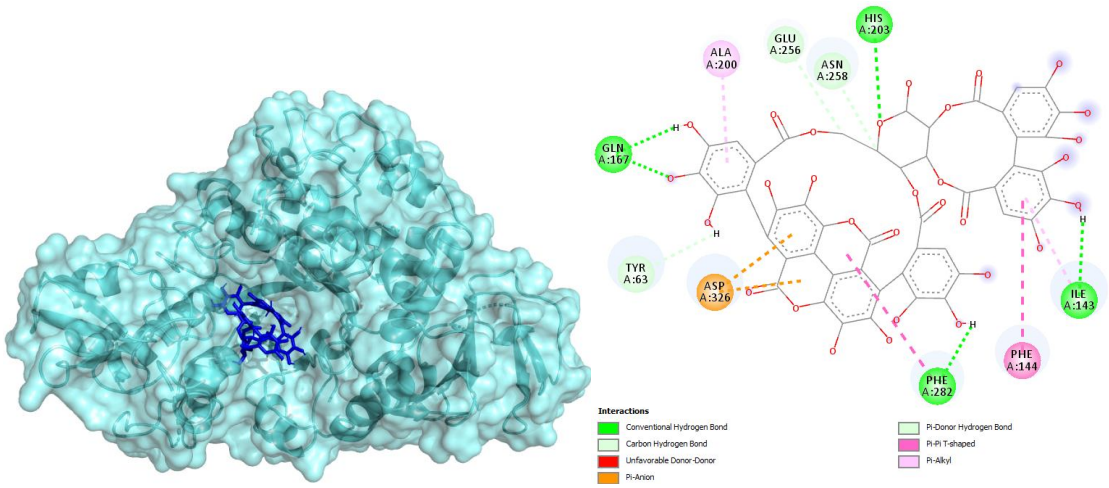

Compound 39

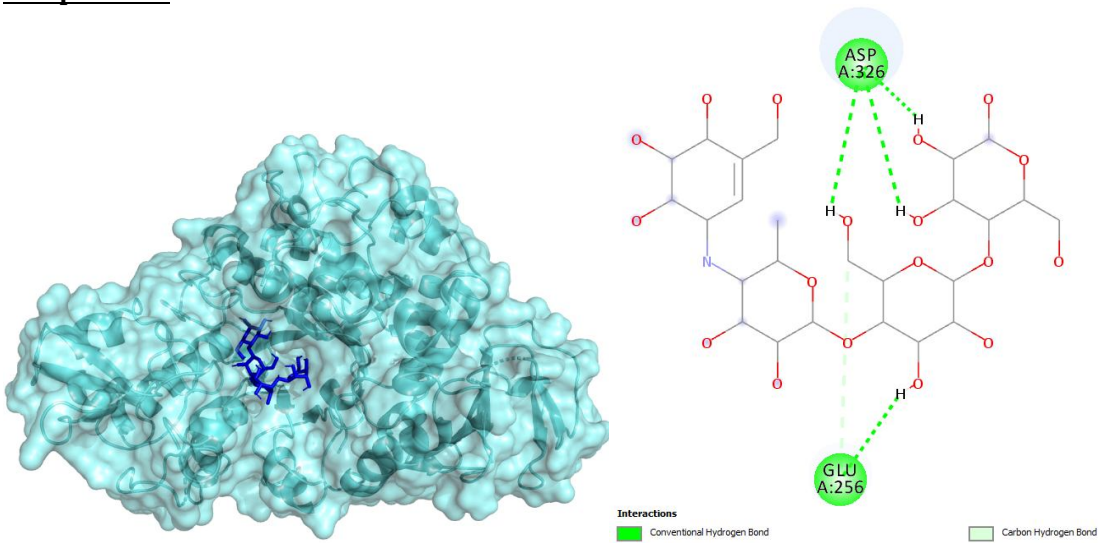

Acarbose

Figure 11: Interaction and binding pose of ligands and control with α-Glucosidase (2ZE0)

5 ligands out of 60 displayed higher binding affinity than the control PT1 with AMP-activated protein kinase (6C9F) in the molecular docking studies. All five were tannins in nature and shared multiple interacting residues with the control PT1. The highest binding affinity was observed in compound 15 (-8.8). These data are presented in table 5.

Table 5: Interaction of ligand library with AMP-activated protein kinase (6C9F)

Ligand	Binding Affinity	Interaction type	Interacting residues
PT1	-8.1	Conventional H bond, Pi-cation, Pi-Pi stacked, Pi-alkyl	ALA 151*, SER 99*, ASN 154*, GLN 124*, LYS 156*, PRO 76*, TYR 277*
C15	-8.8	Conventional H bond, Carbon hydrogen bond, Pi-Pi stacked, Pi-alkyl	HIS 75, TYR 277*, SER 127, LYS 276, GLU 281, LYS 80, ASN 154*, PRO 280, PRO 76*,
C42	-8.6	Conventional H bond, Carbon hydrogen bond, Pi-alkyl	GLU 117, ARG 120, ASN 154*, LYS 156*, PRO 275, PRO 76*, TYR 277*

C17	-8.5	Conventional H bond, Pi-sigma, Pi-Pi stacked, Pi-alkyl	ASP 273, ARG 120, GLN 124*, GLN 123, LYS 156*, ASN 154*, TYR 277*, PRO 76*, PRO 275
C25	-8.3	Conventional H bond, Carbon hydrogen bond, Pi-sigma, Pi-Pi stacked, Pi-alkyl	LYS 43, LYS 156*, GLU 96, TYR 82, TYR 97, SER 99*, ASN 154*, HIS 42, HIS 152, PRO 76*, TYR 277*
C41	-8.2	Conventional H bond, Pi-sigma, Pi-cation, Pi-alkyl	HIS 152, ASP 150, PRO 76*, ASN 154*, GLN 124*, ARG 120, PRO 275

*Interactions common with the control

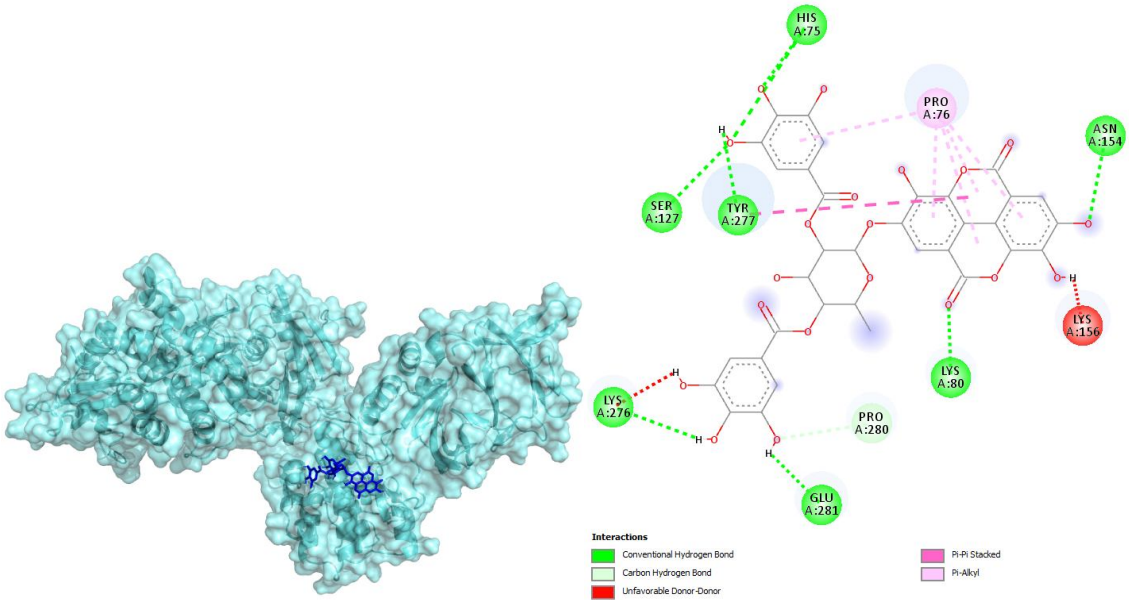

Compound 15

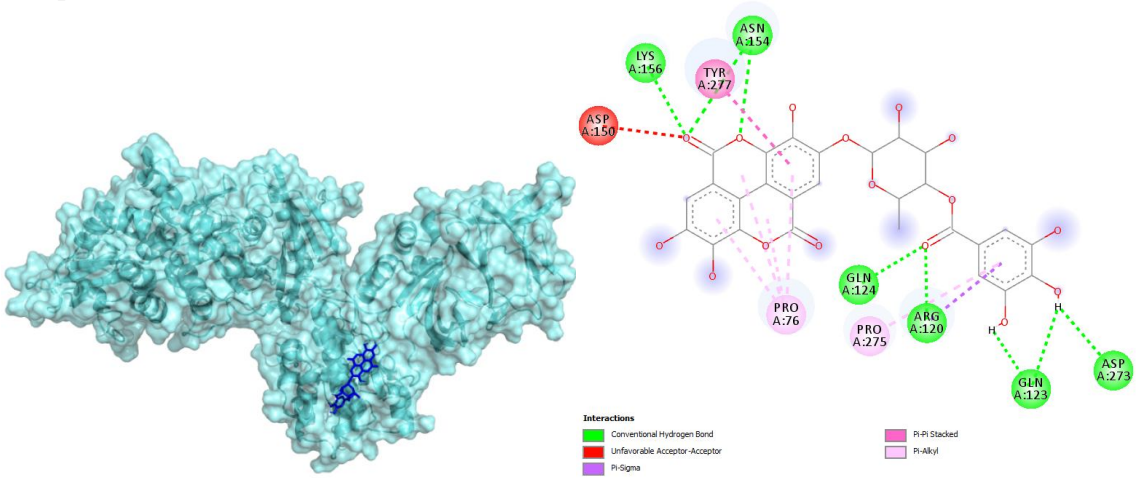

Compound 17

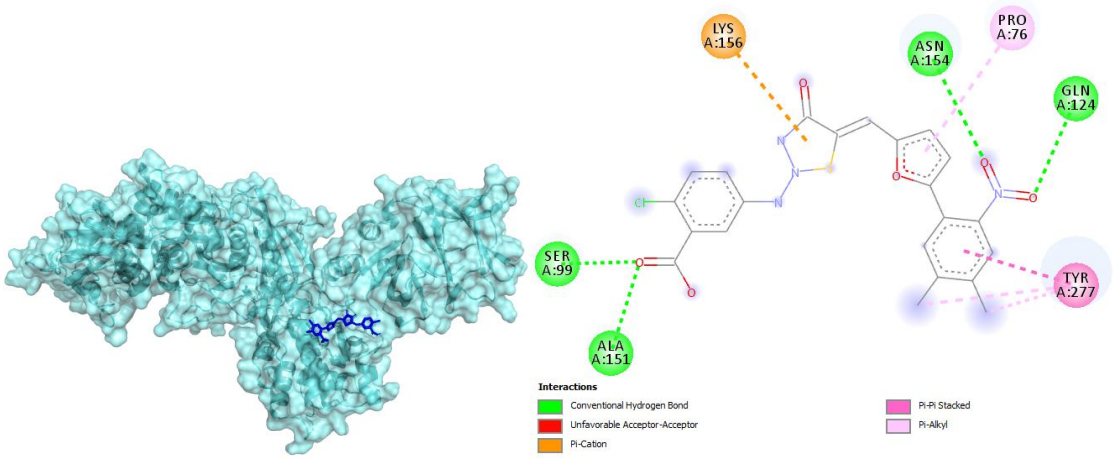

PT1

Figure 12: Interaction and binding pose of ligands and control with AMP-activated Protein Kinase (6C9F)

32 ligands out of 60 displayed a higher binding affinity with dipeptidyl peptidase IV (2G5T) than the control sitagliptin, which had a binding affinity of -8.4. 30 of these were tannins, including the highest binding affinity ligand, compound 42 (-11). All ligands had two or more common interacting residues with the control, except compound 39, which had only one. These data are presented in table 6.

Table 6: Interaction of ligand library with dipeptidyl peptidase IV (2G5T)

Ligand	Binding Affinity	Interaction type	Interacting residues
Sitagliptin	-8.4	Conventional H bond, Carbon hydrogen bond, Halogen (fluorine), Pi-cation, Pi-anion, Pi-donor hydrogen, Pi-Pi stacked, Pi-alkyl	TYR 547*, TYR 666*, TYR 662*, TYR 752*, GLU 206*, GLU 205*, ARG 125*, HIS 740*, SER 630*, GLY 741*, TRP 629*
C42	-11	Conventional H bond, Carbon hydrogen bond, Pi-Pi stacked	LYS 554, GLU 206*, SER 209, GLY 741*, TRP 629*,
C24	-10.6	Conventional H bond, Carbon hydrogen bond, Pi-cation, Pi-alkyl	ASP 545, SER 577, ASN 562, TYR 585, HIS 740*, TYR 547*, GLY 741*, SER 552, LYS 554, ARG 560
C17	-10.5	Conventional H bond, Carbon hydrogen bond, Pi-Pi stacked, alkyl, Pi-alkyl	ASP 709, ARG 125*, TYR 752*, ASP 545, HIS 740*, GLY 741*, SER 630*, ALA 743, TRP 629*
C1	-10.4	Conventional H bond, Carbon hydrogen bond, Pi-cation, Pi-anion, Pi-Pi stacked	TRP 629*, HIS 740*, GLY 741*, ARG 125*, GLU 205*, TYR 631, TYR 662*, TYR 547*, ASP 556, GLU 206*, ASP 545, LYS 554, SER 552
C31	-10.4	Conventional H bond, Pi-cation, Pi-alkyl	ASP 545, GLN 527, ARG 560, TYR 456, GLN 553, ARG 125*, TRP 629*, TYR 547*, ASP 545, LYS 554, PHE 357
C39	-10.4	Conventional H bond, Pi-cation, Pi-Pi stacked, Pi-alkyl	GLN 553, ARG 560, LYS 554, TYR 547*
C15	-10.3	Conventional H bond, Pi-cation, Pi-anion, Pi-Pi stacked, alkyl, Pi-	TYR 547*, TYR 456, TRP 629*, ASP 556, GLN 553, LYS 554, ASP

		alkyl	545, PHE 357
C27	-10.1	Conventional H bond, Pi-anion, Pi-Pi stacked, Pi-Pi T shaped	LYS 554, ASP 556, ARG 560, ARG 669, ARG 125*, TYR 585, GLU 206*, TYR 666*, PHE 357, GLU 205*
C16	-10	Conventional H bond, Carbon hydrogen bond, Pi-donor hydrogen, Pi-alkyl	TYR 662*, TYR 585, TYR 456, ASP 556, ARG 560, ARG 125*, GLU 205*, GLU 206*, SER 552, GLN 553, TRP 629*
C2	-10	Conventional H bond, Carbon hydrogen bond, Pi-Pi stacked, Pi-alkyl	ASP 545, ASP 556, GLN 553, VAL 546, TRP 629*, ARG 125*, TYR 547*, TYR 585, TYR 662*, GLU 206*, LYS 554, TYR 666*
C37	-10	Conventional H bond, Pi-donor hydrogen, Pi-Pi stacked	TYR 456, GLN 553, ARG 560, ARG 125*, GLU 205*, PHE 357, TYR 547*
C41	-10	Conventional H bond, Pi-cation, Pi-Pi stacked	TYR 547*, SER 209, GLU 206*, VAL 207, ASP 556, ARG 4269, PHE 357
C5	-10	Conventional H bond, Carbon hydrogen bond, Pi-cation, Pi-anion, Pi-Pi stacked	GLU 206*, GLN 553, TYR 585, SER 630*, LYS 554, VAL 546, GLY 741*, TYR 547*, HIS 740*, GLU 205*, ARG 125*
C3	-9.9	Conventional H bond, Carbon hydrogen bond, Pi-cation, Pi-anion, Pi-Pi stacked	ASP 545, TRP 629*, GLY 741*, HIS 740*, GLU 206*, TYR 547*, TYR 631, GLU 205*, SER 630*, LYS 554, PHE 357
C6	-9.9	Conventional H bond, Pi-Pi stacked	SER 209, GLU 206*, CYS 551, TYR 585, GLN 553, TYR 547*, ARG 125*, ASN 710, GLU 205*, PHE 357, TRP 629*
C4	-9.8	Conventional H bond, Carbon hydrogen bond, Pi-cation, Pi-donor hydrogen, Pi-Pi stacked	CYS 551, GLN 553, TRP 629*, VAL 546, ARG 125*, LYS 554, PHE 357
C60	-9.8	Conventional H bond, Carbon hydrogen bond, Pi-sigma, Pi-Pi stacked	SER 630*, ARG 125*, TYR 662*, GLU 206*, ARG 669, SER 209, GLU 205*, PHE 357, TYR 547*
C29	-9.6	Conventional H bond, Pi-sigma, Pi-Pi stacked, Pi-alkyl	TYR 547*, SER 630*, ARG 125*, TYR 666*, PHE 357
C32	-9.6	Conventional H bond, Pi-cation	TYR 456, TYR 547*, TYR 585, GLN 553, ARG 560, ARG 669, GLU 206*, TRP 629*, VAL 546, LYS 554
C38	-9.5	Conventional H bond, Pi-Pi stacked, Pi-Pi T shaped	SER 209, GLU 205*, GLU 206*, ARG 669, ARG 125*, LYS 554, ASP 556, TYR 547*, PHE 357
C14	-9.4	Conventional H bond, Pi-cation, Pi-anion, Pi-Pi stacked, Pi-Pi T shaped, Pi-alkyl	ARG 358, VAL 207, TYR 547*, GLU 206*, GLN 553, ARG 125*, GLU 205*, LYS 554, PHE 357
C10	-9.2	Conventional H bond, Carbon hydrogen bond, Pi-cation, Pi-alkyl	ASN 710, GLU 205*, GLY 741*, LYS 554, ARG 125*, HIS 740*, SER 630*
C40	-9.2	Conventional H bond, Pi-Pi stacked, Pi-Pi T shaped	TYR 585, ARG 429, GLN 553, SER 209, GLU 205*, GLU 206*, TYR

			547*, PHE 357
C28	-9.1	Conventional H bond, Pi-cation, Pi-Pi stacked,	ARG 669, GLU 206*, ARG 125*, TYR 547*, HIS 740*, PHE 357
C8	-8.9	Conventional H bond, Carbon hydrogen bond, Pi-cation, Pi-Pi stacked	ASP 545, TRP629, ASN 710, SER 630*, GLU 206*, ARG 125*, TYR 547*, GLN 553, GLY 628, LYS 554
C13	-8.8	Conventional H bond, Carbon hydrogen bond, Pi-Pi stacked, Pi-Pi T shaped	GLN 553, TYR 547*, GLU 205*, GLU 206*, HIS 740*, SER 552, SER 630*
C25	-8.8	Conventional H bond, Pi-cation,	TRP 629*, ASP 545, TYR 662*, ASN 710, ARG 125*, GLU 205*,
C36	-8.8	Conventional H bond, Carbon hydrogen bond, Pi-cation, Pi-anion	SER 209, GLU 205*, TYR 662*, ARG 125*, GLN 553, TRP 629*, GLY 628, GLU 206*, LYS 554
C30	-8.6	Conventional H bond, Pi-cation, Pi-Pi stacked	LYS 554, TRP 629*, ARG 125*, GLU 205*, TYR 547*
C34	-8.6	Conventional H bond, Carbon hydrogen bond, Pi-Pi T shaped	ARG 560, ARG 125*, GLU 205*, GLN 553, SER 630*, HIS 740*, SER 552, TYR 666*
C9	-8.6	Conventional H bond, Pi-anion, Pi-alkyl	GLU 361, GLU 206*, ARG 358, PHE 357, SER 209, TYR 666*,
C57	-8.5	Conventional H bond, Pi-Pi stacked	SER 209, GLU 205*, ARG 125*, HIS 740*, SER 630*, TYR 547*, PHE 357

*Interactions common with the control

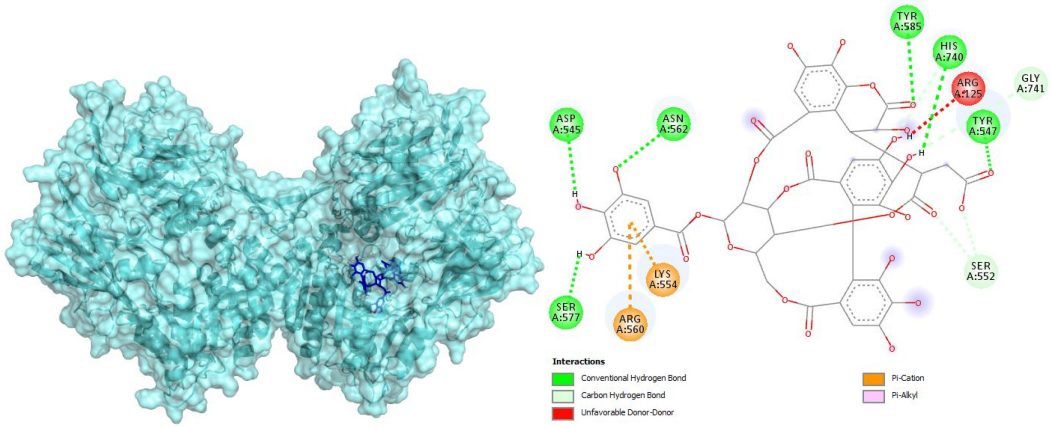

Compound 24

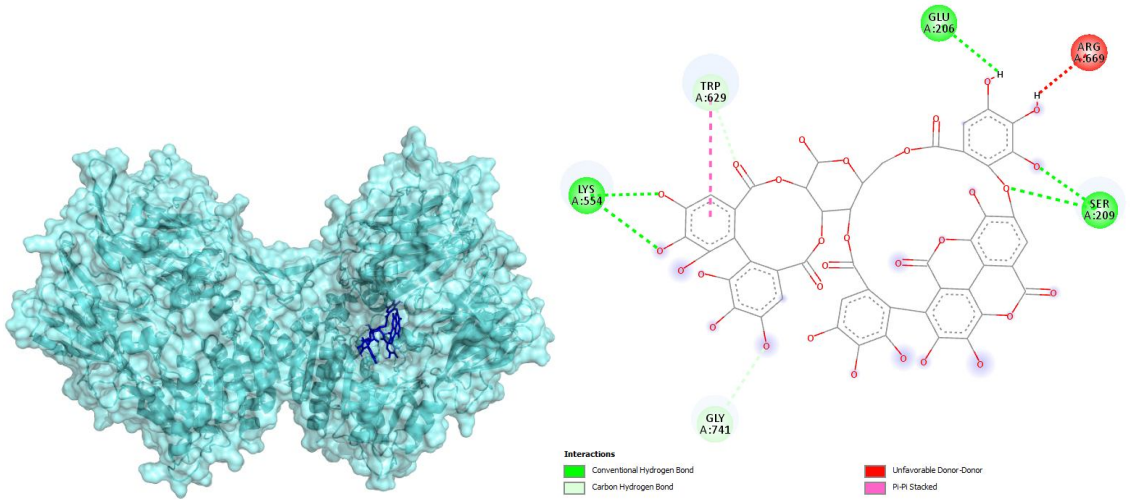

Compound 42

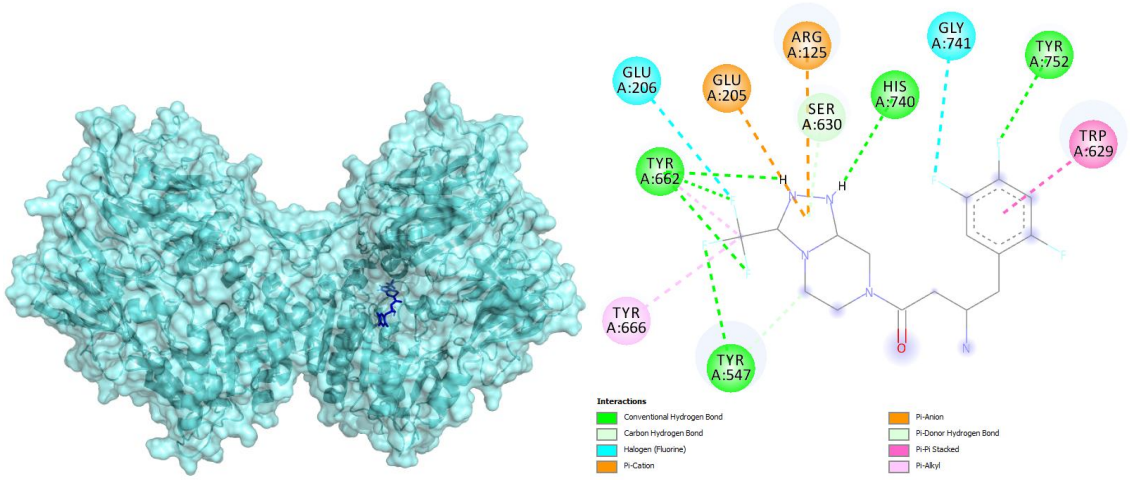

Sitagliptin

Figure 13: Interaction and binding pose of ligands and control with Dipeptidyl Peptidase-IV (2G5T)

2 ligands out of 60 displayed higher binding affinity than the control rosiglitazone with peroxisome proliferator-activated receptor-γ (4EMA) in the molecular docking studies, both of which were tannins. Both shared interacting residues with the control. These data are presented in Table 7.

Table 7: Interaction of ligand library with PPAR-γ (4EMA)

Ligand	Binding Affinity	Interaction type	Interacting residues

Rosiglitazone	-8	Conventional H bond, Pi-Sulfur, Carbon-hydrogen bond, Alkyl, Pi-alkyl, Pi-sigma	CYS285*, ARG288*, SER289*, GLU291*, TYR327*, ILE341*, PHE363*, HIS449*
C10	-8.4	Conventional H bond, Pi-Sulfur, Carbon-hydrogen bond, Pi-anion, Pi-alkyl	LEU255, ARG280, ILE281, GLY284, CYS285*, ARG288*, SER289*, GLU291*, LEU330, SER342, METT364
C6	-8	Conventional H bond, Pi-Sulfur, Pi-Anion, Pi-Pi T-shaped	CYS285*, GLU291*, TYR327*, SER342, MET364

*Interactions common with the control

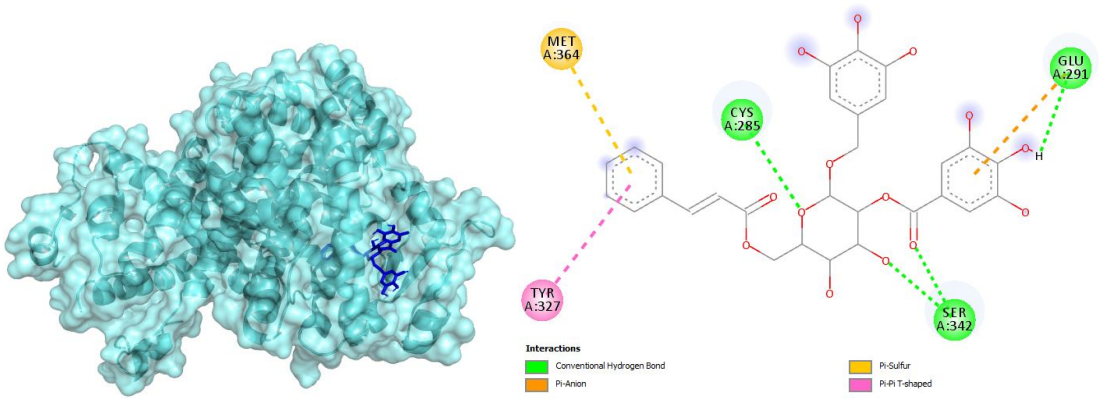

Compound 6

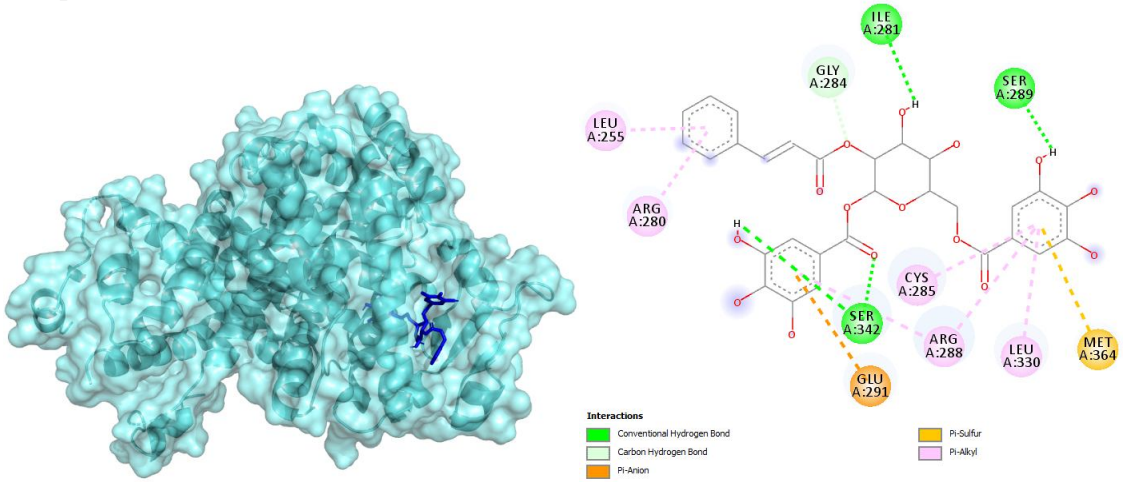

Compound 10

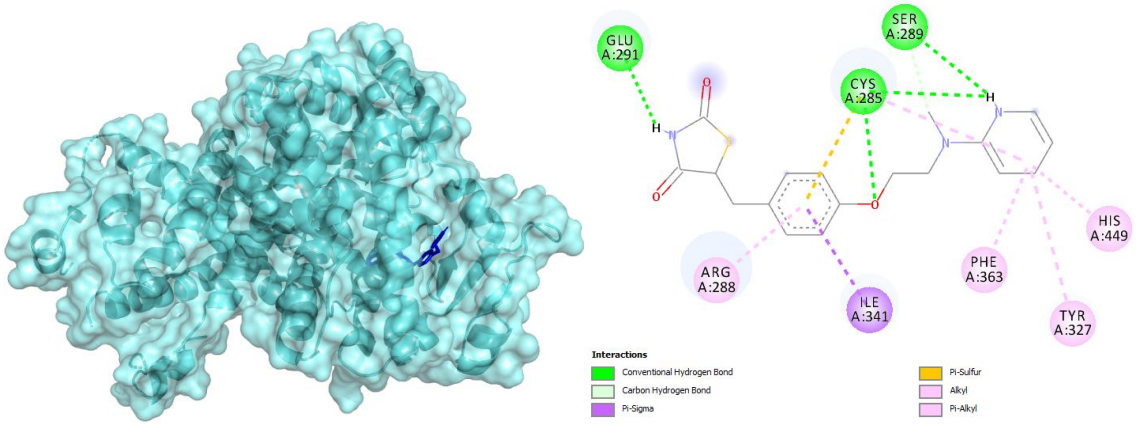

Rosiglitazone

Figure 14: Interaction and binding pose of ligands and control with peroxisome proliferator-activated receptor-γ (4EMA)

The 'SwissADME' and the 'ProTox-II' servers were used to predict the ADMET properties of the phytoconstituents that performed better than the controls in the molecular docking analysis. The 'SwissADME' server evaluated the druglike property of the ligands based on Lipinski's rule of five and Veber's rule amongst other criteria and predicted the GI absorption, BBB permeation, Pgp substrate, CYP inhibition (CYP1A2, CYP2C19, CYP2C9, CYP2D6, CYP3A4), bioavailability score, PAINS alerts, Brenk alerts, lead likeness violations of the ligands. The 'ProTox-II' server predicted the toxicity class, LD50, and organ-specific toxicity generating capabilities of the ligands.

Only four compounds, compounds 18, 47, 58, and 59, were predicted not to violate any rule of Lipinski's rule of five. Compound 46 violated one rule (6 hydrogen bond donors), compounds 9, 11, 46, and 57 violated two rules, and the rest violated three rules. Compounds 58 and 59 had zero violations of Veber's rules, but violations were observed for the rest.

Low GI absorption was predicted for most ligands, save compounds 47, 58, and 59, and no compounds were predicted to have BBB permeation capabilities. Compounds 47 and 59 were predicted to be carcinogenic, while 25, 33, 36, and 59 were deemed to be mutagenic. Immunotoxicity alerts were raised by compounds 14, 24, 25, 27, 37, 38, and 42. All compounds raised the PAINS alert for promiscuity, which is to be expected given the results obtained in the molecular docking studies. The presence of catechol-like structural moieties in most ligands resulted in them triggering the Brenk alert as well.

The obtained data are presented in tables 8 and 9.

Table 8: Druglike properties of ligand library: Lipinski's rule of five, and Veber's rule

ID	Lipinski's rule of five					Veber's rule		
	MW	H-bond donors	H-bond acceptors	LogP	Violations	Rotatable bonds	Polar Surface area	Violations
C58	286.24	4	6	1.86	0	1	111.13	0
C47	302.19	4	8	0.79	0	0	141.34	1
C59	302.24	5	7	1.63	0	1	131.36	0
C18	310.26	5	8	0.59	0	4	144.52	1
C46	322.22	6	9	0.85	1	4	164.75	1

C29	448.33	6	12	1.4	2	2	200.26	1
C57	464.38	8	12	0.94	2	4	210.51	1
C11	484.36	9	14	2.02	2	7	243.9	1
C9	484.36	9	14	0.77	2	7	243.9	1
C17	600.44	8	16	1.3	3	5	267.02	1
C6	600.52	8	14	1.72	3	11	232.9	2
C60	610.52	10	16	0.46	3	6	269.43	1
C10	614.51	8	15	2.17	3	11	249.97	2
C28	634.45	11	18	0.92	3	3	310.66	1
C30	634.45	11	18	0.98	3	6	318.5	1
C7	636.47	11	18	0.52	3	10	310.66	1
C8	636.47	11	18	0.78	3	10	310.66	1
C13	638.48	13	18	1.09	3	9	324.82	1
C25	652.47	9	19	1.19	3	6	313.57	1
C33	670.48	11	20	0.28	3	11	344.8	2
C36	670.48	11	20	0.83	3	11	344.8	2
C15	752.54	10	20	1.77	3	8	333.78	1
C16	752.54	10	20	1.44	3	8	333.78	1
C4	752.63	10	18	2.41	3	14	299.66	2
C40	786.56	13	22	0.89	3	6	377.42	1
C41	786.56	13	22	0.83	3	6	377.42	1
C3	788.57	13	22	1.54	3	13	377.42	2
C5	788.57	13	22	1.42	3	13	377.42	2
C2	874.71	12	21	1.41	3	15	357.19	2
C23	936.65	16	26	0.11	3	4	455.18	1
C1	940.68	15	26	0.25	3	16	444.18	2
C24	954.66	13	27	-0.91	3	5	447.09	1
C27	956.68	13	27	0.85	3	12	447.09	2
C14	972.68	15	28	0.04	3	10	478.32	1
C34	974.69	15	28	0.31	3	17	478.32	2
C12	988.72	14	28	0.48	3	18	467.32	2
C37	1084.72	18	30	0.23	3	1	529.76	1
C38	1084.72	18	30	-1.15	3	1	529.76	1
C39	1084.72	17	30	-0.38	3	0	518.76	1
C42	1084.72	16	30	1.14	3	0	507.76	1

Table 9: ADMET properties of ligand library: GI absorption, BBB permeation, Pgp substrate, CYP inhibition (CYP1A2, CYP2C19, CYP2C9, CYP2D6, CYP3A4), Predicted Toxicity Class (Class I: fatal if swallowed, Class II: fatal if swallowed, Class III: toxic if swallowed, Class IV: harmful if swallowed, Class V: may be harmful if swallowed, Class VI: non-toxic), Predicted LD50 (mg/kg), Predicted Toxicity, Bioavailability Score, PAINS alerts, Brenk alerts, Leadlikeness violations

ID	GI absorption	BBB permeation	Pgp substrate	CYP inhibition (out of 5)	Predicted Toxicity Class	Predicted LD50 (mg/kg)	Predicted Toxicity	Bioavailability Score	PAINS alerts	Brenk alerts	Leadlikeness violations
C58	High	No	No	3	5	3919	-	0.55	1	1	0
C47	High	No	No	1	4	2991	Carcinogenicity	0.55	1	3	0
C59	High	No	No	3	3	159	Carcinogenicity, Mutagenicity	0.55	1	1	0
C18	Low	No	No	0	4	1960	-	0.56	1	1	0
C46	Low	No	No	1	5	2260	-	0.11	1	2	0
C29	Low	No	No	0	5	5000	-	0.17	1	3	1
C57	Low	No	No	0	5	5000	-	0.17	1	1	1
C9	Low	No	No	0	5	2260	-	0.17	1	2	1
C11	Low	No	No	0	5	2260	-	0.17	1	2	1
C17	Low	No	No	0	5	2190	-	0.17	1	3	1
C6	Low	No	Yes	0	5	5000	-	0.17	1	3	2
C60	Low	No	Yes	0	5	5000	-	0.17	1	1	1
C10	Low	No	Yes	0	5	5000	-	0.17	1	3	2
C28	Low	No	Yes	0	5	2260	-	0.17	1	2	1
C30	Low	No	Yes	0	5	3000	-	0.17	1	3	1
C7	Low	No	Yes	0	5	2260	-	0.17	1	2	2
C8	Low	No	Yes	0	5	2260	-	0.17	1	2	2
C13	Low	No	Yes	0	5	2260	-	0.17	1	3	2
C25	Low	No	Yes	0	4	823	Immunotoxicity, Mutagenicity	0.11	1	3	1
C33	Low	No	No	0	4	600	Mutagenicity	0.11	1	2	2
C36	Low	No	No	0	4	600	Mutagenicity	0.11	1	2	2
C15	Low	No	No	0	5	2190	-	0.17	1	4	2
C16	Low	No	No	0	5	2190	-	0.17	1	4	2
C4	Low	No	No	0	5	5000	-	0.17	1	3	2
C40	Low	No	Yes	0	5	2190	-	0.17	1	2	1
C41	Low	No	Yes	0	5	2260	-	0.17	1	2	1
C3	Low	No	Yes	0	5	2260	-	0.17	1	2	2

C5	Low	No	Yes	0	5	2260	-	0.17	1	2	2
C2	Low	No	Yes	0	5	5000	-	0.17	1	3	3
C1	Low	No	Yes	0	5	2260	-	0.17	1	2	3
C24	Low	No	Yes	0	4	420	Immunotoxicity	0.11	1	3	1
C27	Low	No	Yes	0	4	823	Immunotoxicity	0.11	1	3	2
C14	Low	No	Yes	0	2	7	Immunotoxicity	0.11	1	2	2
C34	Low	No	Yes	0	4	600	-	0.11	1	2	2
C12	Low	No	Yes	0	4	600	-	0.11	1	2	2
C37	Low	No	Yes	0	4	1213	Immunotoxicity	0.17	1	4	1
C38	Low	No	Yes	0	4	1213	Immunotoxicity	0.17	1	4	1
C39	Low	No	Yes	0	5	5000	-	0.17	1	4	1
C42	Low	No	Yes	0	4	1000	Immunotoxicity	0.17	1	4	1

Discussion

Diabetes has become a serious public health concern affecting a large portion of the global population. As the treatment by synthetic drugs is often limited due to their unfavorable pharmacokinetic properties and side effects, there is a significant need to enhance the range of therapeutic palliatives and make them available to all kinds of patients (Haque & Begum, 2011). With this intention, this study evaluated the antidiabetic activity of *Terminalia Chebula* in rat model. Alloxan is extensively used to induce DM in animal models due to its relative price and availability (Federiuk *et al.*, 2004; GOLDNER & GOMORI, 1944; Cruz *et al.*, 1961).

In Figure 1, it is apparent that the body weight of the alloxan-induced diabetic rats increased significantly after the administration of *Terminalia Chebula* extract that imitated the weight-gaining pattern as showed by the negative control group. Other plants of the genus *Terminalia* have also been reported for similar activity. Several scientists have reported that the extracts of *Terminalia catappa* ameliorate alloxan-induced lowering of body weight in murine models. (Ahmed *et al.*, 2005; Hayaza *et al.*, 2019; Nagappa *et al.*, 2003) *Terminalia superba, Terminalia bellirica,* and *Terminalia paniculata* extracts have also been documented for their activity against diabetes-induced weight loss in murine models. (Gupta *et al.*, 2020; Kamtchouing *et al.*, 2006; Ramachandran *et al.*, 2012) Moreover, the findings in this study were parallel to several prior studies where the administration of *Aloe megalacantha Baker* extract, *Sigesbeckia orientalis, Panicum maximum, Anacardium occidentale L, Ricinus communis, Chloroxylon swietenia, Persea americana,* and *Tithonia diversifolia* resulted in a similar outcome (Zhang *et al.*, 2016; Asif *et al.*, 2016; E *et al.*, 2012; Gad-Elkareem *et al.*, 2019; Ramana *et al.*, 2017; Yetendje *et al.*, 2019; Yuneldi *et al.*, 2018). The extract of *T. chebula* performed better in this regard than *Calpurnia aurea* leaves (Belayneh, 2018).

In Figure 2, significant decreases in blood glucose levels were observed after the administration of *T. chebula* extract at low, medium, and high doses in alloxan-induced diabetic rats. The gradual decline in blood glucose levels was similar to that of metformin, but the latter was observed to be more effective than the test extract (*T. chebula*) at the same dose. As the test extract was unpurified and therefore contained less of the active glucose-lowering component(s), this was deemed justified. Reduction of blood glucose level was observed to be dose-dependent for both test extract and metformin. As seen in the graph, a large dose (650mg) of the test extract induced a rapid reduction in blood glucose levels, but a moderate dose (250 mg) caused a more gradual response. The sole administration of the plant

extract or the control drug to non-alloxan induced groups did not cause significant fluctuations compared to the negative control group, and all curves obtained thereby were found to overlap with the negative control curve, indicating that neither the drug nor the plant is to be associated with any harmful effects. This blood-glucose level lowering activity is common to several other plants of the genus, including *Terminalia catappa, Terminalia brownie, Terminalia pallida,* etc.; all of which have been reported to exert the aforementioned effect in alloxan or streptozotocin-indiced diateic rats or mice (Alema *et al*., 2020; Hayaza *et al*., 2019; Nagappa *et al.*, 2003; Rao *et al*., 2003). Additionally, *Calpurnia aurea* leaves, *Zizyphusmauritiana, Aloe megalacantha* bark extract *Sigesbeckia orientalis, Panicum maximum, Anacardium occidenta*le L, *Ricinus communis, Chloroxylon swietenia, persea americana, Catharentus roseus, Eucalyptus globulus, Sargassum longiotom, Streblus asper,* and *Sedum adenotrichum* also displayed identical outcomes in previous studies (Federiuk *et al*., 2004; GOLDNER & GOMORI, 1944; Cruz *et al*., 1961; Asif *et al*., 2016; Gad-Elkareem *et al*., 2019; Ramana *et al*., 2017; Yetendje *et al*., 2019; Yuneldi *et al*., 2018; Belayneh, 2018; Yadav & Kumar, 2014; D'AMOUR & Smith, 1941; Hammeso *et al*., 2019; Kannan *et al*., 2012; Jaiswal *et al*., 2017).

In Figure 3, treatment of alloxan-induced rats with metformin or test extract resulted in a reduction in SGPT levels. This response varied depending on the doses of test extract and metformin. However, the overall lowering effect of metformin was slightly higher than the test extract. When compared to the negative control group, the SGPT levels of the other six non-alloxan treated groups did not differ significantly, ruling out the possibilities of serious side effects from both metformin and the plant. Similar effects were observed in the cases of *Terminalia paniculate, Terminalia arjuna,* and *Terminalia bellerica* from the same genus (Biswas *et al*., 2011; MdR *et al.*, 2021; Ramachandran *et al*., 2012).

Figure 4 depicts a significant increase in SGOT levels after the rats were administered alloxan. In alloxan-induced diabetic rats, a progressive reduction in SGOT level was detected following the administration of metformin and test extract at three distinct doses (low, medium, and high). Groups treated solely with metformin or the test extract showed no substantial changes in SGOT values as opposed to the negative control group and therefore were considered safe in this regard. Other *Terminalia* plants, namely *Terminalia paniculate, Terminalia arjuna,* and *Terminalia bellerica* have been reported for having the same therapeutic effects (Biswas *et al*., 2011; MdR *et al*., 2021; Ramachandran *et al*., 2012).

In **Figure 5**, alloxan administration raised plasma creatinine to a level higher than the negative control. The alloxan-mediated elevation of plasma creatinine was reversed after the administration of the test extract in low, medium, and high doses. Although groups treated with metformin exhibited a similar trend in creatinine level declination, the effects were slightly stronger than the test extract. *Ricinus communis, Anacardium occidentale* L, *Chloroxylon swietenia, Zizyphus mauritiana, Persea americana, Eucalyptus globules, Catharentus roseus,* and *Sedum adenotrichum* extracts were also observed to have a similar effect on plasma creatinine levels (Gad-Elkareem *et al*., 2019; Ramana *et al*., 2017; Yetendje *et al*., 2019; Jaiswal *et al*., 2017; Jarald *et al*., 2009; Naz *et al*., 2019).

In **Figure 6**, in both treatment groups, it was observed that the high dose of drugs produced a more prominent effect. The metformin and test extract treatment groups had nearly identical response patterns. However, metformin-treated groups had a slightly better prognosis. The total cholesterol levels obtained from the other non-alloxan-influenced groups were observed to be similar to those obtained from the negative control group, nullifying the risk of significant adverse effects following drug or plant administration. Similar outcomes were observed in prior studies conducted on *Sigesbeckia orientalis, Chloroxylon swietenia, Zizyphusmauritian,* and *Sedum adenotrichum* (Asif *et al*., 2016; Ramana *et al*., 2017; Jarald *et al*., 2009; Naz *et al*., 2019).

In **figure 7**, it was recorded that the HDL values in the negative control group were approximately equal to the groups receiving either metformin or test extract. In the case of *Milletia aboensis*, a similar finding was reported by Minaopunye and Bassey, 2015 (Minaopunye & Bassey, 2015).

In **Figure 8**, LDL readings in groups receiving metformin or test extract only were similar to those in the negative control group, indicating no significant risk of adverse effects from oral ingestion of either. The declination of LDL levels in diabetic rats was slightly more noticeable in the metformin-treated groups than in test extract-treated groups. Identical results have previously been reported for *Anacardium occidentale* L., *Chloroxylon swietenia*, *Streblus asper*, and *Forsythia suspense* (Zhang *et al*., 2016; Ramana *et al*., 2017; Jaiswal *et al*., 2017; Karan *et al*., 2013).

In **Figure 9,** alloxan conditioning resulted in a sharp spike in the triglyceride levels, but both metformin and the test extract reversed this dose-dependently. The performance of metformin was slightly better than the test extract in this regard. Sole administration of metformin or the test extract in all three doses resulted in triglyceride levels almost similar to the negative control, indicating the safety of both substances in this regard. These findings were consistent with data from previous experimentations conducted on *Chloroxylon swietenia* and *Anacardium occidentale* L. (Ramana *et al*., 2017; Jaiswal *et al*., 2017).

In alloxan-treated rats, the damaging effects of alloxan resulted in cellular atrophy and a reduction in body weight. The effect of the extract on this change was similar to the metformin control group in diabetic rats, albeit the weight loss was prevented to a greater degree by the test extract. However, in the non-diabetic rats, administration of metformin resulted in a slight reduction of body weight for all three doses, while the test extract-treated group displayed an increase in body weight. This suggests that the hypoglycemic effect of the extract was not, in any way, mediated through the loss of appetite; rather, despite sufficient food intake, the test extract yielded a pronounced anti-hyperglycemic effect.

The blood insulin levels in groups 6, 7, and 8, i.e., the test extract-treated diabetic groups, were observed to be significantly higher. Moreover, the hepatic glycogen content increased significantly in rats from these groups, further cementing and solidifying the idea that the extract acted as an insulin secretagogue. These findings suggest that the test extract's antidiabetic activity may be propagated through enhanced insulin secretion. *T.chebula* has previously been found to aid in glucose absorption and carbohydrate metabolism in another investigation (Periasamy *et al*., 2006).

The *in silico* studies presented a unique insight into the mechanism of action of the extract. Most ligands from the *T. chebula* fruit constituent ligand library were predicted to have low GI absorption, and only a handful satisfied Lipinski's rule of five or Veber's rule. However, a considerable number of ligands showed high affinity to the enzymes α-amylase and α-glucosidase, 34 for the first and 44 for the second, and the majority of these were tannins, 29 in case of the first and 38 for the second. Large tannin-type molecule-mediated inhibition of these macromolecular targets has already been documented, and therefore it is highly likely that the antidiabetic effect of the extract, at least partially, is exerted through the inhibition of these enzymes (Toda *et al*., 2001; Tundis *et al*., 2010). Apart from α-amylase and α-glucosidase, DPP-IV was the antidiabetic drug target that displayed high ligand-binding energies and favorable interactions with a large number of assayed ligands. 32 ligands of the library displayed a higher binding energy with this target than the control sitagliptin (binding energy: -8.4), of which 30 were tannins. Compounds 1,3-di-O-galloyl-β-D-glucose, eschweilenol C, and isoquercetin (compounds 9, 29, and 57 respectively) were considered the most likely to exert the DPP-IV mediated activity, as these compounds were of relatively lower molecular weight and had fewer Lipinski's rules violations (2 each). Isoquercetin's antidiabetic activity has also been observed in prior studies, and eschweilenol C containing

Punica granatum fruit has been reported for its antidiabetic Activity (Jayachandran *et al*., 2018; Thanh *et al*., 2019; R. Zhang *et al*., 2011). Moreover, none of these compounds were predicted to induce any sort of toxicity and were found to be relatively safe. Further research on these compounds is warranted as research on these may yield potential lead compounds for DPP-IV inhibition.

Another plant of the same genus, *T. arjuna*, contains various chemicals, including flavonoids and tri-terpenoids, which have a strong affinity for alpha-amylase and alpha-glucosidase. Phytoconstituents from its extract adhere synergistically to those receptors. Insulin sensitivity, higher glucose assimilation rate, and stimulation of glucose uptake by affinity peripheral tissue are all potential outcomes of this process. Moreover, diabetogenic alloxan produces free radicals that cause tissue damage, and antioxidant components may serve as free radical scavengers, conferring activity toward lipid peroxidation, OH•, and O2. •. *T. chebula* has already been reported to have certain antioxidant properties, and this may very well play a part in its antidiabetic effect, as the concentration of alloxan-free radicals may decrease after administration of the extract, and subsequent damage may be mitigated. However, this assumption needs further research-backed justification. Our studies show that an increase in insulin secretion may be a potential mode of action by which our extract imparts its antidiabetic activity. The inhibition of α-amylase and α-glucosidase may also be key to the test extracts antidiabetic activity. A more thorough investigation is required to justify all conceivable mechanisms of action for *T. chebula*'s antidiabetic activity, as a more comprehensive understanding may lead to the discovery of novel antidiabetic compounds (Journal *et al*., 2014; Miaffo *et al*., 2019; Morshed *et al*., 2011).

Conclusion

This study demonstrates that *T. chebula* fruit extract potentially influences a number of physiological pathways to exert its antidiabetic activity. Moreover, in the diseased state, pathological changes to multiple biological parameters such as creatinine, lipid profile, SGPT, and SGOT levels were significantly ameliorated by both the plant extract and metformin. Apart from these desirable changes, all the biological parameters of rats belonging to non-diabetic groups remain unchanged after treatment with either the plant extract or metformin. This safety profile was reflected *in silico*, as most constituents of the plant were predicted to be safe. Moreover, molecular docking studies indicated that the inhibition of macromolecules α-amylase, α-glucosidase, and DPP-IV might be responsible for the activity. While the plant should be deemed to be of high potential, the exact constituents that exert antidiabetic activity are yet to be determined *in vitro* and *in vivo*, though our *in silico* studies should help shed some light in that general direction. In conclusion, a comprehensive and thorough investigation of *T. chebula* and its constituents may lead to its inclusion in the diabetes management system in the future.

References

Afsana, A., Karim, A., Alramadan, M. J., Habib, S. H., & Ali, L. (n.d.). Type 2 diabetes mellitus in Bangladesh a prevalence based cost-of-illness study (2019). *Bio Med Care Health Serv Res*, *19*(1).

Afshari, A. R., Sadeghnia, H. R., & Mollazadeh, H. (2016). A review on potential mechanisms of Terminalia chebula in Alzheimer's disease. *Advances in Pharmacological Sciences*, *2016*.

Ahmed, S. M., Vrushabendra, S. B. M., Gopkumar, P., Dhanapal, R., & Chandrashekara, V. M. (2005). *Anti-diabetic activity of Terminalia catappa*

Linn. leaf extracts in alloxan-induced diabetic rats.

Akhtar, H., & Husain, S. Z. (2019). A Descriptive Review on Traditional Herbal Drug-Terminalia Chebula. *Journal of Advanced Research in Biochemistry and Pharmacology*, *2*(1), 21–28.

Akram, N., Srivastava, M., & Mishra, M. K. (2019). Antidiabetic Activity of root of Terminalia chebula on alloxan induced diabetic rat. *World J Pharm Med Res*, *5*(3), 108–112.

Alam, S., Alam, A., Quamri, M. A., Sofi, G., & Khan, M. Q. (2020). *A brief review of Halelajat (Terminalia chebula) in Unani medicine*. *0*(0).

Alema, N. M., Periasamy, G., Sibhat, G. G., Tekulu, G. H., & Hiben, M. G. (2020). Antidiabetic activity of extracts of Terminalia brownii Fresen. Stem bark in mice. *Journal of Experimental Pharmacology*, *12*, 61.

Amalraj, A., & Gopi, S. (2017). Medicinal properties of Terminalia arjuna (Roxb.) Wight & Arn.: A review. In *Journal of Traditional and Complementary Medicine* (Vol. 7, Issue 1, pp. 65–78). National Taiwan University. https://doi.org/10.1016/j.jtcme.2016.02.003

Anil, M., & Nandini, P. (2010). Simultaneous isolation and identification of phytoconstituents from Terminalia chebula by preparative chromatography. *Journal of Chemical and Pharmaceutical Research*, *2*(5), 97–103.

Asif, M., Saleem, M., Yousaf, S., Saadullah, M., Zafar, M., Khan, R. U., & Yuchi, A. (2016). *Antidiabetic activity of aqueous extract of Sigesbeckia orientalis (St . Paul ' s Wort) in alloxan-induced diabetes model*. 1–10.

Aung, E. P. P., Lwin, S. H., Aye, N. N., & Phyu, K. P. (2017). Hypoglycemic Effect of Terminalia chebula retz. Fruit on alloxan-induced diabetic rats. *Siriraj Medical Journal*, *69*(2), 80–84.

Bag, P. K., Roy, N., Acharyya, S., Saha, D. R., Koley, H., Sarkar, P., & Bhowmik, P. (2019). In vivo fluid accumulation-inhibitory, anticolonization and anti-inflammatory and in vitro biofilm-inhibitory activities of methyl gallate isolated from Terminalia chebula against fluoroquinolones resistant Vibrio cholerae. *Microbial Pathogenesis*, *128*, 41–46.

Banerjee, P., Eckert, A. O., Schrey, A. K., & Preissner, R. (2018). ProTox-II: a webserver for the prediction of toxicity of chemicals. *Nucleic Acids Research*, *46*(W1), W257–W263.

Basha, S. J., & Code, Q. R. (2017). A review on Terminalia chebula. *IJPR*, *7*(10).

Belayneh, Y. M. (2018). *Antidiabetic Activities of Hydromethanolic Leaf Extract of Calpurnia aurea (Ait .) Benth . Subspecies aurea (Fabaceae) in Mice*. *2018*.

Berman, H., Henrick, K., & Nakamura, H. (2003). Announcing the worldwide protein data bank. *Nature Structural & Molecular Biology*, *10*(12), 980.

Biswas, M., Kar, B., Bhattacharya, S., Kumar, R. B. S., Ghosh, A. K., & Haldar, P. K. (2011). Antihyperglycemic activity and antioxidant role of Terminalia arjuna leaf in streptozotocin-induced diabetic rats.

Pharmaceutical Biology, *49*(4), 335–340.

Charan, J., & Kantharia, N. D. (2013). How to calculate sample size in animal studies? *Journal of Pharmacology & Pharmacotherapeutics*, *4*(4), 303.

Daina, A., Michielin, O., & Zoete, V. (2017). SwissADME: a free web tool to evaluate pharmacokinetics, drug-likeness and medicinal chemistry friendliness of small molecules. *Scientific Reports*, *7*(1), 1–13.

Dallakyan, S., & Olson, A. J. (2015). Small-molecule library screening by docking with PyRx. In *Chemical biology* (pp. 243–250). Springer.

Das, G., Kim, D.-Y., Fan, C., Gutiérrez-Grijalva, E. P., Heredia, J. B., Nissapatorn, V., Mitsuwan, W., Pereira, M. L., Nawaz, M., & Siyadatpanah, A. (2020). Plants of the genus Terminalia: An insight on its biological potentials, pre-clinical and clinical studies. *Frontiers in Pharmacology*, *11*.

Design, L. (2014). *Pharmacophore and ligand-based design with Biovia Discovery Studio®*.

E, O. J., S, A. B., & A, U. J. (2012). Antidiabetic activities of ethanolic extract and fraction of Anthocleista djalonensis. *Asian Pacific Journal of Tropical Biomedicine*, *2*(6), 461–464. https://doi.org/10.1016/S2221-1691(12)60076-8

Federiuk, I. F., Casey, H. M., Quinn, M. J., Wood, M. D., & Ward, K. W. (2004). Induction of type-1 diabetes mellitus in laboratory rats by use of alloxan: route of administration, pitfalls, and insulin treatment. *Comparative Medicine*, *54*(3), 252–257.

Gad-Elkareem, M. A. M., Abdelgadir, E. H., Badawy, O. M., & Kadri, A. (2019). Potential antidiabetic effect of ethanolic and aqueous-ethanolic extracts of Ricinus communis leaves on streptozotocin-induced diabetes in rats. *PeerJ*, *7*, e6441.

GOLDNER, M. G., & GOMORI, G. (1944). Studies on the mechanism of alloxan diabetes. *Endocrinology*, *35*(4), 241–248.

Guex, N., & Peitsch, M. C. (1997). SWISS□MODEL and the Swiss□Pdb Viewer: an environment for comparative protein modeling. *Electrophoresis*, *18*(15), 2714–2723.

Gulam, S. M., Palaian, S., Emirates, U. A., & Kumar, M. (2019). *UNCOMMON SIDE EFFECTS OF COMMONLY USED ANTI-DIABETICS : TIME TO*. *10*(September). https://doi.org/10.13040/IJPSR.0975-8232.10(9).4145-48

Gupta, A., Kumar, R., & Pandey, A. K. (2020). Antioxidant and antidiabetic activities of Terminalia bellirica fruit in alloxan induced diabetic rats. *South African Journal of Botany*, *130*, 308–315.

Halgren, T. A. (1996). Merck molecular force field. I. Basis, form, scope, parameterization, and performance of MMFF94. *Journal of Computational Chemistry*, *17*(5□6), 490–519.

Hammeso, W. W., Emiru, Y. K., Getahun, K. A., & Kahaliw, W. (2019). *Antidiabetic and Antihyperlipidemic Activities of the Leaf Latex Extract of*

Aloe megalacantha Baker (Aloaceae) in Streptozotocin-Induced Diabetic Model. *2019*.

Hanwell, M. D., Curtis, D. E., Lonie, D. C., Vandermeersch, T., Zurek, E., & Hutchison, G. R. (2012). Avogadro: an advanced semantic chemical editor, visualization, and analysis platform. *Journal of Cheminformatics*, *4*(1), 1–17.

Haque, A., & Begum, R. (2011). *Anti-hyperglycemic and lipid lowering effect of Terminalia arjuna Bark extract on Streptozotocin induced Type-2 Diabetic Model Rats EXTRACT ON STREPTOZOTOCIN INDICED TYPE 2 DIABETIC MODEL RATS*. *June 2014*.

Hasan, T., & Sultana, M. (2018). Antidiabetic potency of Bangladeshi medicinal plants. *J Ayurvedic Herb Med*, *4*(1), 35–42.

Hayaza, S., Istiqomah, S., Susilo, R. J. K., Inayatillah, B., Ansori, A. N. M., Winarni, D., Husen, S. A., & Darmanto, W. (2019). Antidiabetic activity of ketapang (Terminalia catappa L.) leaves extract in streptozotocin-induced diabetic mice. *Indian Vet J*, *96*(12), 11–13.

Hosamani, K. M. (1994). Terminalia chebula seed oil—a minor source of 12□hydroxyoctadec□cis□9□enoic acid: Natural products as a source for the food and agricultural industries. *Journal of the Science of Food and Agriculture*, *64*(3), 275–277.

Hospital, S. (1961). *Effect of Intra-arterial Insulin on Tissue Cholesterol and Fatty Acids in Alloxan-Diabetic Dogs*. *IX*(January).

Jaiswal, Y. S., Tatke, P. A., Gabhe, S. Y., & Vaidya, A. B. (2017). Journal of Traditional and Complementary Medicine Antidiabetic activity of extracts of Anacardium occidentale Linn . leaves on n -streptozotocin diabetic rats. *Journal of Traditional Chinese Medical Sciences*, *7*(4), 421–427. https://doi.org/10.1016/j.jtcme.2016.11.007

Jarald, E. E., Joshi, S. B., & Jain, D. C. (2009). *Antidiabetic activity of extracts and fraction of Antidiabetic activity of extracts and fraction of Zizyphus mauritiana*. *0209*. https://doi.org/10.1080/13880200902752488

Jayachandran, M., Zhang, T., Ganesan, K., Xu, B., & Chung, S. S. M. (2018). Isoquercetin ameliorates hyperglycemia and regulates key enzymes of glucose metabolism via insulin signaling pathway in streptozotocin-induced diabetic rats. *European Journal of Pharmacology*, *829*, 112–120.

Jhong, C., Riyaphan, J., Lin, S., Chia, Y., & Weng, C. (2015). S creening alpha□glucosidase and alpha□amylase inhibitors from natural compounds by molecular docking in silico. *Biofactors*, *41*(4), 242–251.

Journal, A., Thomson, H. A. J., Ojo, O. O., & Peter, R. (2014). *Aqueous Bark Extracts of Terminalia Arjuna Stimulates Insulin Release , Enhances Insulin Action and Inhibits Starch Digestion and Protein Glycation in Vitro*. *1*(1), 1–6.

Juang, L., Sheu, S., & Lin, T. (2004). Determination of hydrolyzable tannins in the fruit of Terminalia chebula Retz. by high□performance liquid

chromatography and capillary electrophoresis. *Journal of Separation Science*, *27*(9), 718–724.

Kamtchouing, P., Kahpui, S. M., Dzeufiet, P.-D. D., Tédong, L., Asongalem, E. A., & Dimo, T. (2006). Anti-diabetic activity of methanol/methylene chloride stem bark extracts of Terminalia superba and Canarium schweinfurthii on streptozotocin-induced diabetic rats. *Journal of Ethnopharmacology*, *104*(3), 306–309.

Kannan, V. R., Rajasekar, G. S., Rajesh, P., Balasubramanian, V., Ramesh, N., Solomon, E. K., Nivas, D., & Chandru, S. (2012). Anti-diabetic Activity on Ethanolic Extracts of Fruits of. *American Journal of Drug Discovery and Development*, *2*(3), 135–142.

Karan, S. K., Mondal, A., Mishra, S. K., Pal, D., Karan, S. K., Mondal, A., Mishra, S. K., & Pal, D. (2013). *Antidiabetic effect of Streblus asper in streptozotocin-induced diabetic rats. 0209*. https://doi.org/10.3109/13880209.2012.730531

Kim, H. G., Cho, J.-H., Jeong, E. Y., Lim, J. H., Lee, S. H., & Lee, H. S. (2006). Growth-inhibiting activity of active component isolated from Terminalia chebula fruits against intestinal bacteria. *Journal of Food Protection*, *69*(9), 2205–2209.

Kim, S., Chen, J., Cheng, T., Gindulyte, A., He, J., He, S., Li, Q., Shoemaker, B. A., Thiessen, P. A., Yu, B., Zaslavsky, L., Zhang, J., & Bolton, E. E. (2021). PubChem in 2021: new data content and improved web interfaces. *Nucleic Acids Research*, *49*(D1), D1388–D1395. https://doi.org/10.1093/nar/gkaa971

Kumar, B. S., Lakshman, K., Jayaveera, K. N., Krishna, N. V., Manjunath, M., Suresh, M. V, Reddy, H., & Naik, S. (2009). Estimation of rutin and quercetin in Terminalia chebula by HPLC. *Asian Journal of Research in Chemistry*, *2*(4), 388–389.

Lee, D. Y., Kim, H. W., Yang, H., & Sung, S. H. (2017). Hydrolyzable tannins from the fruits of Terminalia chebula Retz and their α-glucosidase inhibitory activities. *Phytochemistry*, *137*, 109–116.

LIN, T., NONAKA, G., NISHIOKA, I., & HO, F. (1990). Tannins and Related Compounds. CII.: Structures of Terchebulin, an Ellagitannin Having a Novel Tetraphenylcarboxylic Acid (Terchebulic Acid) Moiety, and Biogenetically Related Tannins from Terminalia chebula RETZ. *Chemical and Pharmaceutical Bulletin*, *38*(11), 3004–3008.

MdR, T., Jannat, B., Mostafa, A., Purni, F. A., & Khondoker, S. (2021). An Evaluation of Diabetes Ameliorating Capacity of Terminalia bellerica Ethanolic Extract on Alloxan-Induced Diabetic Rat Including Safety Profile Study. *J Clin Mol Endocrinol*, *6*, 1–33.

Miaffo, D., Kamgue, O. G., Tebou, N. L., Maa, C., Temhoul, M., & Kamanyi, A. (2019). *Antidiabetic and antioxidant potentials of Vitellaria paradoxa barks in alloxan-induced diabetic rats.*

Minaopunye, O. B., & Bassey, E. E. (2015). *Evaluation of Anti-Diabetic and Anti-lipidemic Activities of Aqueous Leaf Extract of Millettia aboensis and Its Effect on Pancreatic Histology of Alloxan-Induced Diabetic Rats*. *3*(2), 24–29. https://doi.org/10.11648/j.ab.20150302.11

Mohiuddin, G. S., Palaian, S., Shankar, P. R., Sam, K. G., & Kumar, M. (2019). Uncommon side effects of commonly used anti-diabetics: time to monitor them. *International Journal of Pharmaceutical Sciences and Research*, *10*(9), 4145–4148.

Morshed, M. A., Haque, A., Rokeya, B., & Ali, L. (2011). *ANTI - HYPERGLYCEMIC AND LIPID LOWERING EFFECT OF TERMINALIA ARJUNA BARK EXTRACT ON STREPTOZOTOCIN INDICED TYPE 2 DIABETIC MODEL RATS*. *3*(4).

Nabeno, M., Akahoshi, F., Kishida, H., Miyaguchi, I., Tanaka, Y., Ishii, S., & Kadowaki, T. (2013). A comparative study of the binding modes of recently launched dipeptidyl peptidase IV inhibitors in the active site. *Biochemical and Biophysical Research Communications*, *434*(2), 191–196.

Nagappa, A. N., Thakurdesai, P. A., Rao, N. V., & Singh, J. (2003). Antidiabetic activity of Terminalia catappa Linn fruits. *Journal of Ethnopharmacology*, *88*(1), 45–50.

Naz, D., Muhamad, A., Zeb, A., & Shah, I. (2019). *In vitro and in vivo Antidiabetic Properties of Phenolic Antioxidants From Sedum adenotrichum*. *6*(November), 1–7. https://doi.org/10.3389/fnut.2019.00177

Nigam, M., Mishra, A. P., Ibrahim, A., Mahadi, D., Achyut, H., Tarun, A., & Devkota, H. P. (2020). *Fruits of Terminalia chebula Retz .: A review on traditional uses , bioactive chemical constituents and pharmacological activities*. *August 2019*, 1–16. https://doi.org/10.1002/ptr.6702

O'Boyle, N. M., Banck, M., James, C. A., Morley, C., Vandermeersch, T., & Hutchison, G. R. (2011). Open Babel: An open chemical toolbox. *Journal of Cheminformatics*, *3*(1), 1–14.

Pang, T., Zhang, Z.-S., Gu, M., Qiu, B.-Y., Yu, L.-F., Cao, P.-R., Shao, W., Su, M.-B., Li, J.-Y., & Nan, F.-J. (2008). Small molecule antagonizes autoinhibition and activates AMP-activated protein kinase in cells. *Journal of Biological Chemistry*, *283*(23), 16051–16060.

Patel, D. K., Kumar, R., Prasad, S. K., Sairam, K., & Hemalatha, S. (2011). Antidiabetic and in vitro antioxidant potential of Hybanthus enneaspermus (Linn) F. Muell in streptozotocin–induced diabetic rats. *Asian Pacific Journal of Tropical Biomedicine*, *1*(4), 316–322.

Patel, D. K., Prasad, S. K., Kumar, R., & Hemalatha, S. (2012). An overview on antidiabetic medicinal plants having insulin mimetic property. *Asian Pacific Journal of Tropical Biomedicine*, *2*(4), 320–330.

Periasamy, G., Kumar, S., Arulselvan, P., Kumar, D. S., & Subramanian, S. P. (2006). *Anti-Diabetic Activity of Fruits of Terminalia chebula on Streptozotocin Induced Diabetic Rats*. *52*(3), 283–291.

Prakash, S. D. V, Satya, S. N., & Vangalapati, M. (2012). Purification of Chebulinic acid from Terminalia chebula species by column chromatography. *Journal of Chemical, Biological and Physical Sciences (JCBPS)*, *2*(4), 1753.

Pugazhendhi, A., Shafreen, R. B., Devi, K. P., & Suganthy, N. (2018). Assessment of antioxidant, anticholinesterase and antiamyloidogenic effect of Terminalia chebula, Terminalia arjuna and its bioactive constituent 7-methyl gallic acid–an in vitro and in silico studies. *Journal of Molecular Liquids*, *257*, 69–81.

Rahman, M., Uddin, M., Reza, A. S. M., Tareq, A. M., Emran, T. Bin, & Simal-Gandara, J. (2021). Ethnomedicinal value of antidiabetic plants in bangladesh: A comprehensive review. *Plants*, *10*(4), 729.

Ramachandran, S., Rajasekaran, A., & Manisenthilkumar, K. T. (2012). Investigation of hypoglycemic, hypolipidemic and antioxidant activities of aqueous extract of Terminalia paniculata bark in diabetic rats. *Asian Pacific Journal of Tropical Biomedicine*, *2*(4), 262–268.

Ramana, S., Kadali, M., Das, M. C., Vijayaraghavan, R., & Kumar, M. V. (2017). *Evaluation of Antidiabetic Activity of Aqueous and Ethanolic Extracts of Leaves of Chloroxylon Swietenia in Streptozotocin (STZ) Induced Diabetes in Albino Rats*. *10*(3), 1347–1353.

Ramesh, B., Karuna, R., Sreenivasa, R. S., Haritha, K., Sai, M. D., Sasis, B. R. B., & Saralakumari, D. (2012). Effect of Commiphora mukul gum resin on hepatic marker enzymes, lipid peroxidation and antioxidants status in pancreas and heart of streptozotocin induced diabetic rats. *Asian Pacific Journal of Tropical Biomedicine*, *2*(11), 895–900.

Rao, B. K., Sudarshan, P. R., Rajasekhar, M. D., Nagaraju, N., & Rao, C. A. (2003). Antidiabetic activity of Terminalia pallida fruit in alloxan induced diabetic rats. *Journal of Ethnopharmacology*, *85*(1), 169–172.

Sawant, R. L., Wadekar, J. B., Kharat, S. B., & Makasare, H. S. (2018). Targeting PPAR-γ to design and synthesize antidiabetic thiazolidines. *EXCLI Journal*, *17*, 598.

Schrödinger, LLC. (2015). *The {PyMOL} Molecular Graphics System, Version~1.8*.

Sgpt, P., & Rats, M. (2018). *Biosaintifika*. *10*(3), 519–525.

Shivanagoudra, S. R., Perera, W. H., Perez, J. L., Athrey, G., Sun, Y., Jayaprakasha, G. K., & Patil, B. S. (2019). Cucurbitane-type compounds from Momordica charantia: Isolation, in vitro antidiabetic, anti-inflammatory activities and in silico modeling approaches. *Bioorganic Chemistry*, *87*, 31–42.

Singh, Ankit, & Sheikh, J. (2020). Cleaner functional dyeing of wool using Kigelia Africana natural dye and Terminalia chebula bio-mordant. *Sustainable Chemistry and Pharmacy*, *17*, 100286.

Singh, Anurag, Srivastav, R., & Pandey, A. K. (2018). Effect of the seeds of

Terminalia chebula on blood serum, lipid profile and urine parameters in STZ induced diabetic rats. *Journal of Pharmacognosy and Phytochemistry*, *7*(2), 1–5.

Sivamaruthi, B. S., Ramkumar, V. S., Archunan, G., Chaiyasut, C., & Suganthy, N. (2019). Biogenic synthesis of silver palladium bimetallic nanoparticles from fruit extract of Terminalia chebula–In vitro evaluation of anticancer and antimicrobial activity. *Journal of Drug Delivery Science and Technology*, *51*, 139–151.

Smith, L. (1941). *A METhOD FOR*.

Sotoudeh, R., Mousa-Al-Reza Hadjzadeh, Z. G., & Aghaei, A. (2019). The anti-diabetic and antioxidant effects of a combination of Commiphora mukul, Commiphora myrrha and Terminalia chebula in diabetic rats. *Avicenna Journal of Phytomedicine*, *9*(5), 454.

Tariq, A. L., & Reyaz, A. L. (2013). Quantitative phytochemical analysis of traditionally used medicinal plant Terminalia chebula. *Int Res J Biotechnol*, *4*(5), 101–105.

Thanh, H. N., Huyen, N. T., Van Khanh, N., Thu, D. K., & Tung, B. T. (2019). Phytochemicals and antidiabetic activity of the aqueous extract of the Punica granatum fruit in streptozotocin-induced diabetic mice. *Journal of Basic and Clinical Physiology and Pharmacology*, *30*(4).

Toda, M., Kawabata, J., & Kasai, T. (2001). Inhibitory effects of ellagi-and gallotannins on rat intestinal α-glucosidase complexes. *Bioscience, Biotechnology, and Biochemistry*, *65*(3), 542–547.

Tundis, R., Loizzo, M. R., & Menichini, F. (2010). Natural products as α-amylase and α-glucosidase inhibitors and their hypoglycaemic potential in the treatment of diabetes: an update. *Mini Reviews in Medicinal Chemistry*, *10*(4), 315–331.

van Gunsteren, W. F., Billeter, S. R., Eising, A. A., Hünenberger, P. H., Krüger, P., Mark, A. E., Scott, W. R. P., & Tironi, I. G. (1996). Biomolecular simulation: the GROMOS96 manual and user guide. *Vdf Hochschulverlag AG an Der ETH Zürich, Zürich*, *86*, 1–1044.

Wild, S., Roglic, G., Green, A., Sicree, R., & King, H. (2004). Global prevalence of diabetes: estimates for the year 2000 and projections for 2030. *Diabetes Care*, *27*(5), 1047–1053.

Yadav, D., & Kumar, N. (2014). Nanonization of curcumin by antisolvent precipitation: Process development, characterization, freeze drying and stability performance. *International Journal of Pharmaceutics*, *477*(1–2), 564–577. https://doi.org/10.1016/j.ijpharm.2014.10.070

Yetendje, L. C., Sedar, G., Njateng, S., & Dongmo, A. A. (2019). IN VIVO ANTIDIABETIC ACTIVITY AND MECHANISM OF ACTION. *International Journal of Research -GRANTHAALAYAH*, *7*(8), 415–430. https://doi.org/10.29121/granthaalayah.v7.i8.2019.695

Yin, P., Wang, Y., Yang, L., Sui, J., & Liu, Y. (2018). *Hypoglycemic Effects in*

Alloxan-Induced Diabetic Rats of the Phenolic Extract Enriching Ellagic Acid, Kaempferol and Their Derivatives from Mongolian Oak Cups.

Zhang, R., Yao, Y., Wang, Y., & Ren, G. (2011). Antidiabetic activity of isoquercetin in diabetic KK-A y mice. *Nutrition & Metabolism*, *8*(1), 1–6.

Zhang, Y., Feng, F., Chen, T., Li, Z., & Shen, Q. W. (2016). Author ' s Accepted Manuscript. *Journal of Ethnopharmacology*. https://doi.org/10.1016/j.jep.2016.07.002